J|A|C|S ARTICLES

Published on Web 09/09/2009

Neighboring Amide Participation in Thioether Oxidation: Relevance to Biological Oxidation

Richard S. Glass,*,† Gordon L. Hug,*,‡ Christian Schöneich,*,§ George S. Wilson,*,|| Larisa Kuznetsova,† Tang-man Lee,† Malika Ammam,|| Edward Lorance,⊥ Thomas Nauser,# Gary S. Nichol,† and Takuhei Yamamoto†

Departments of Chemistry, The University of Arizona, Tucson, Arizona 85721, The University of Kansas, Lawrence, Kansas 66047, Radiation Laboratory, University of Notre Dame, Notre Dame, Indiana 46556, Vanguard University, Costa Mesa, California 92626, Department of Pharmaceutical Chemistry, University of Kansas, Lawrence, Kansas 66047 and the Institute of Inorganic Chemistry, Department of Chemistry and Applied Biosciences, ETH Zürich, 8093 Zürich, Switzerland

Received June 15, 2009; E-mail: rglass@u.arizona.edu

Abstract: To investigate neighboring amide participation in thioether oxidation, which may be relevant to brain oxidative stress accompanying β-amyloid peptide aggregation, conformationally constrained methylthionorbornyl derivatives with amido moieties were synthesized and characterized, including an X-ray crystallographic study of one of them. Electrochemical oxidation of these compounds, studied by cyclic voltammetry, revealed that their oxidation peak potentials were less positive for those compounds in which neighboring group participation was geometrically possible. Pulse radiolysis studies provided evidence for bond formation between the amide moiety and sulfur on one-electron oxidation in cases where the moieties are juxtaposed. Furthermore, molecular constraints in spiro analogues revealed that S−O bonds are formed on one-electron oxidation. DFT calculations suggest that isomeric σ^*_{SO} radicals are formed in these systems.

Introduction

The thioether side chain of methionine in peptides and proteins is susceptible to oxidation. Indeed methionine is one of the most easily oxidized residues by reactive oxygen species.[1] Such oxidation is of great interest because of its relevance to inactivation of protein pharmaceuticals,[2] aging,[3] cataract formation,[4] and neurodegenerative diseases such as Parkinson's[5] and Alzheimer's.[6] Oxidation of methionine to methionine sulfoxide results in converting a hydrophobic side chain into a hydrophilic one. Therefore, it is not surprising that this change has important consequences for protein folding/unfolding, degradation, inactivation[7] and aggregation.[8] Such oxidation has also been suggested[1,9] to play a regulatory role. It has been suggested[10] that methionine residues can protect against oxidative stress by being selectively oxidized and even catalytically by being reduced back[11] after oxidation. One-electron oxidation of methionine in β-amyloid peptides may play a role in the pathogenesis of Alzheimer's disease.[12−18] Since Met-35 in

† Department of Chemistry, The University of Arizona.
‡ Radiation Laboratory, University of Notre Dame.
§ Department of Pharmaceutical Chemistry, University of Kansas.
|| Department of Chemistry, The University of Kansas.
⊥ Department of Chemistry, Vanguard University.
Institute of Inorganic Chemistry, ETH Zürich.

(1) Vogt, W. *Free Radical Biol. Med.* **1995**, *18*, 93–105.
(2) Meyer J. D.; Ho, B.; Manning, M. C. In *Rational Design of Stable Protein Formulations*; Carpenter, J. F., Manning M. C., Eds.; Kluwer: New York, 2002; pp 85−108.
(3) (a) Stadtman, E. R.; Van Remmen, H.; Richardson, A.; Wehr, N. B.; Levine, R. L. *Biochim. Biophys. Acta* **2005**, *1703*, 135–140. (b) Stadtman, E. R. *Free Rad. Res.* **2006**, *40*, 1250–1258.
(4) Karunakaran-Datt, A.; Kennepohl, P. *J. Am. Chem. Soc.* **2009**, *131*, 3577–3582.
(5) (a) Hokenson, M. J.; Uversky, V. N.; Goers, J.; Yamin, G.; Munishkina, L. A.; Fink, A. L. *Biochemistry* **2004**, *43*, 4621–4633. (b) Wassef, R.; Haenold, R.; Hansel, A.; Brot, N.; Heinemann, S. H.; Hoshi, T. *J. Neurosci.* **2007**, *27*, 12808–12816.
(6) Ciccotosto, G. D.; Barnham, K. J.; Cherny, R. A.; Masters, C. L.; Bush, A. I.; Curtain, C. C.; Cappai, R.; Tew, D. *Lett. Pept. Sci.* **2003**, *10*, 413–417.
(7) (a) Pan, B.; Abel, J.; Ricci, M. S.; Brems, D. N.; Wang, D. I. C.; Trout, B. L. *Biochemistry* **2006**, *45*, 15430–15443. (b) Thirumangalathu, R.; Krishnam, S.; Bondarenko, P.; Speed-Ricci, M.; Randolph, T. W.; Carpenter, J. F.; Brems, D. N. *Biochemistry* **2007**, *46*, 6213–6224, and references therein. (c) Buré, C.; Goffinot, S.; Delmas, A. F.; Cadene, M.; Culard, F. *J. Mol. Biol.* **2008**, *376*, 120–130.
(8) Breydo, L.; Bocharova, O. N.; Makarava, N.; Salnikov, V. V.; Anderson, M.; Baskakov, I. V. *Biochemistry* **2005**, *44*, 15534–15543.
(9) Ciorba, M. A.; Heinemann, S. H.; Weisbach, H.; Brot, N.; Hoshi, T. *Proc. Natl. Acad. Sci. U.S.A.* **1997**, *94*, 9932–9937.
(10) (a) Stadtman, E. R. *Arch. Biochem. Biophys.* **2004**, *423*, 2–5. (b) Sideri, T. C.; Willetts, S. A.; Avery, S. V. *Microbiology* **2009**, *155*, 612–623. (c) Luo, S.; Levine, R. L. *FASEB J.* **2009**, *23*, 464–472.
(11) Reduction of methionine sulfoxide residues to methionine is catalyzed by the enzymes msrA for the S-epimer and msrB for the R-epimer at sulfur: Boschi-Mueller, S.; Gand, A.; Branlant, G. *Arch. Biochem. Biophys.* **2008**, *474*, 266–273.
(12) Schöneich, C. *Biochim. Biophys. Acta* **2005**, *1703*, 111–119.
(13) Selkoe, D. J. *Ann. Intern. Med.* **2004**, *140*, 627–638.
(14) Selkoe, D. J. *Ann. Med.* **1989**, *21*, 73–76. Selkoe, D. J. *Physiol. Rev.* **2001**, *81*, 741–766.
(15) Yankner, B. A.; Duffy, L. K.; Kirschner, D. A. *Science* **1990**, *250*, 279–282. Davis, J.; van Nostrand, W. E. *Proc. Natl. Acad. Sci. U.S.A.* **1996**, *93*, 2996–3000. Walsh, D. M.; Klyubin, I.; Fadeeva, J. V.; Cullen, W. K.; Anwyl, R.; Wolfe, M. S.; Rowan, M. J.; Selkoe, D. J. *Nature* **2002**, *416*, 535–539.
(16) Butterfield, D. A. *Curr. Med. Chem.* **2003**, *10*, 2651–2659. Bush, A. I. *Trends Neurosci.* **2003**, *26*, 207–214.

Aβ(1−42) is critical for causing oxidative stress,[19] electron-transfer from sulfur of this residue was cited as a key for initiating metal-ion-dependent production of reactive oxygen species.[20] Aβ Peptides and especially their Cu(II) complexes were found to produce hydrogen peroxide[20,21] and a mechanism for this reaction was recently proposed[22] based on theoretical studies. This requires reduction of Cu(II) to Cu(I) and then reaction with oxygen. Electrochemical reduction of Aβ−Cu(II) produces Aβ−Cu(I), which reacts with oxygen to yield H_2O_2.[23,24] Reduction of Cu(II) to Cu(I) followed by a "Fenton-type" reaction[25] would generate a hydroxyl radical which would oxidize proteins. It was pointed out that the redox potentials for methionine oxidation and Cu(II) reduction result in a thermodynamically unfavorable electron-transfer process.[26] Furthermore the originally proposed peak potential for Aβ−Cu(II), $E_{pa} \approx +0.80$ V vs NHE,[21b] was redetermined to be substantially less positive, $E_{pa} \approx +0.36$ V vs NHE,[23] rendering the redox reaction even less favorable. Addition of methionine to Aβ(1−16/20)−Cu(II) was reported not to result in reduction of the Cu(II).[27] The Cu(I) complexes of Aβ peptides produced by ascorbate reduction were shown to generate $^{\bullet}$OH in the presence of hydrogen peroxide[28] and Cu(II)−Aβ complexes with added reducing agents can catalytically generate $^{\bullet}$OH. The lack of reduction of Aβ-Cu(II) by added methionine was cited as evidence refuting the involvement of Met-35 in Aβ(1−42) as a reducing agent.[27] However, methionine may not be a good model for Met-35 in Aβ peptide oligomers because of possible neighboring group participation in the peptide oligomer. Stabilization of the sulfur radical cation by amide moieties and the C-terminal carboxylate ion in Met-peptides has been reported.[25,29] Based on modeling studies, the amide carbonyl group of Ile-31 is close to the sulfur of Met-35 and it was proposed to stabilize the corresponding sulfur radical cation by bond formation,[31] that is, neighboring group participation.[32] However, neighboring group participation in the oxidation of thioethers not only stabilizes the corresponding sulfur radical cation, but may also render the oxidation potential of thioethers less positive, that is, easier to oxidize. For example, 1,5-dithiocane (**1**) undergoes reversible oxidation with a peak potential of +0.34 V vs Ag/0.1 M $AgNO_3$ in CH_3CN[33] whereas aliphatic thioethers show irreversible oxidation in acetonitrile with peak potentials of 1.1 to 1.7 V vs the same reference electrode.[34] Indeed the oxidation potential of **1** is sufficiently cathodic that it is oxidized by Cu(II).[35] Both the stability of the radical cation and dication of **1** and its lowered oxidation potential are ascribed to neighboring group participation, that is, transannular S−S bond formation.[36] Nevertheless, theoretical calculations on models for S∴O two-center, three-electron (2c-3e) bond formation involving methionine in peptide environments in water found no lowering of $E°$ as a result of such interaction.[37] However, in a previous survey, we reported[38] that thioether-amide **2a**, in which neighboring group participation is geometrically possible, undergoes irreversible oxidation electrochemically in acetonitrile with a peak potential less positive by 550 mV than that of **2b**, in which neighboring amide participation is precluded owing to molecular constraints. Furthermore, calculations support the formation of a σ*-type 2c-3e bond between S and O in the radical cation of **2a**.[31,37] In view of the relevance of these results to the proposed mechanism for the pathogenesis of Alzheimer's disease outlined above as well as the oxidation of methionine containing peptides and proteins, in general, the reinvestigation and expanded study of neighboring amide participation in thioether oxidation reported here was undertaken. The aims of this study were several-fold: (1) to establish that oxidation of **2a** occurs with neighboring amide participation using the technique of pulse radiolysis;[39] (2) to establish unequivocally that O-participation rather than N-participation can occur by using further conformation constraints and to explore whether preorganization further lowers the oxidation potential; (3) to determine the effect of the electron-

(17) Boyd-Kimball, D.; Sultana, R.; Poon, H. F.; Lynn, B. C.; Casamenti, F.; Pepeu, G.; Klein, J. B.; Butterfield, D. A. *Neuroscience* **2005**, *132*, 313–324. Butterfield, D. A.; Lauderback, C. M. *Free Radical Biol. Med.* **2002**, *32*, 1050–1060. Varadarajan, S.; Yatin, S.; Aksenova, M.; Butterfield, D. A. *J. Struct. Biol.* **2000**, *130*, 184–208.

(18) Butterfield, D. A.; Drake, J.; Pocernich, C.; Castegna, A. *Trends Mol. Med.* **2001**, *7*, 548–554. Butterfield, D. A. *Free Rad. Res.* **2002**, *36*, 1307–1313. Butterfield, D. A. *Curr. Med. Chem.* **2003**, *10*, 2651–2659.

(19) Varadarajan, S.; Yatin, S.; Kanski, J.; Jahanshahi, F.; Butterfield, D. A. *Brain Res. Bull.* **1999**, *50*, 133–141. Atwood, C. S.; Perry, G.; Zeng, H.; Kato, Y.; Jones, W. D.; Ling, K.-Q.; Huang, X.; Moir, R. D.; Wang, D.; Sayre, L. M.; Smith, M. A.; Chen, S. G.; Bush, A. I. *Biochemistry* **2004**, *43*, 560–568.

(20) Butterfield, D. A. *Chem. Res. Toxicol.* **1997**, *10*, 495–506. Sayre, L. M.; Zagorski, M. G.; Surewicz, W. K.; Krafft, G. A.; Perry, G. *Chem. Res. Toxicol.* **1997**, *10*, 518–526. Butterfield, D. A.; Kanski, J. *Peptides* **2002**, *23*, 1299–1309. Butterfield, D. A.; Boyd-Kimball, D. *Biochim. Biophys. Acta* **2005**, *1703*, 149–156. Ali, F. E.; Separovic, F.; Barrow, C. J.; Cherny, R. A.; Fraser, F.; Bush, A. I.; Masters, C. L.; Barnham, K. J. *J.Peptide Sci.* **2005**, *11*, 353–360.

(21) (a) Huang, X.; Atwood, C. S.; Hartshorn, M. A.; Multhap, G.; Goldstein, L. E.; Scarpa, R. C.; Cuajungco, M. P.; Gray, D. N.; Lim, J.; Moir, R. D.; Tanzi, R. E.; Bush, A. I. *Biochemistry* **1999**, *38*, 7609–7616. (b) Huang, X.; et al. *J. Biol. Chem.* **1999**, *274*, 37111–37116. (c) Opazo, C.; Huang, X.; Cherny, R. A.; Moir, R. D.; Roher, A. E.; White, A. R.; Cappai, R.; Masters, C. L.; Tanzi, R. E.; Inestrosa, N. C.; Bush, A. I. *J. Biol. Chem.* **2002**, *277*, 40302–40308. (d) Del Rio, M. J.; Velez-Pardo, C. *Curr. Med. Chem. Centr. Nerv. Sys. Agents* **2004**, *4*, 279–285.

(22) Hewitt, N.; Rauk, A. *J. Phys. Chem. B* **2009**, *113*, 1202–1209.

(23) Jiang, D.; Men, L.; Wang, J.; Zhang, Y.; Chickenyen, S.; Wang, Y.; Zhou, F. *Biochemistry* **2007**, *46*, 9270–9282.

(24) For H_2O_2 production from chemically prepared AβCu(I) see: Himes, R. A.; Park, G. Y.; Siluvai, S.; Blackburn, N. J.; Karlin, K. C. *Angew. Chem., Int. Ed.* **2008**, *47*, 9084–9087.

(25) Liochev, S. I. In *Metal Ions in Biological Systems*; Sigel, A., Sigel, H., Eds.; Marcel Dekker: New York, 1999; Vol. 36, pp 1−39. Burkitt, M. J. *Prog. React. Kinetic Mech.* **2003**, *28*, 75–103. Prousek, J. *Pure Appl. Chem.* **2007**, *79*, 2325–2338.

(26) Schöneich, C. *Arch. Biochem. Biophys.* **2002**, *397*, 370–376.

(27) da Silva, G. F. Z.; Lykourinou, V.; Angerhofer, A.; Ming, L.-J. *Biochim. Biophys. Acta* **2009**, *1792*, 49–55.

(28) Guilloreau, L.; Combalbert, S.; Sournia-Saquet, A.; Mazarguil, H.; Faller, P. *ChemBio Chem* **2007**, *8*, 1317–1325.

(29) (a) Schöneich, C.; Pogocki, D.; Wisniowski, P.; Hug, G. L.; Bobrowski, K. *J. Am. Chem. Soc.* **2000**, *122*, 10224–10225. (b) Varadarajan, S.; Kanski, J.; Aksenova, M.; Lauderback, C.; Butterfield, D. A. *J. Am. Chem. Soc.* **2001**, *123*, 5625–5631. (c) Schöneich, C.; Pogocki, D.; Hug, G. L.; Bobrowski, K. *J. Am. Chem. Soc.* **2003**, *125*, 13700–13713.

(30) Pogocki, D.; Schöneich, C. *Chem. Res. Toxicol.* **2002**, *15*, 408–418.

(31) Pogocki, D.; Serdiuk, K.; Schöneich, C. *J. Phys. Chem. A* **2003**, *107*, 7032–7042.

(32) Glass, R. S. In *Sulfur-centered Reactive Intermediates in Chemistry and Biology*; Chatgiliagoglu, C., Asmus, K.-D., Eds.; NATO ASI Series Vol. 197; Plenum: London, 1990; pp 227−238.

(33) Wilson, G. S.; Swanson, D. D.; King, J. T.; Glass, R. S.; Ryan, M. D.; Musker, W. K. *J. Am. Chem. Soc.* **1979**, *101*, 1040–1042. Ryan, M. D.; Swanson, D. D.; Glass, R. S.; Wilson, G. S. *J. Phys. Chem.* **1981**, *85*, 1069–1075.

(34) Coleman, B. R.; Glass, R. S.; Setzer, W. N.; Prabhu, U. D. G.; Wilson, G. S. *Adv. Chem. Ser.* **1982**, *201*, 417–441.

(35) Musker, W. K.; Wolford, T. L.; Roush, P. B. *J. Am. Chem. Soc.* **1978**, *100*, 6416–6421.

(36) (a) Asmus, K.-D. *Acc. Chem. Res.* **1979**, *12*, 436–442. (b) Musker, W. K. *Acc. Chem. Res.* **1980**, *13*, 200–206. (c) Brown, T. G.; Hirschon, A. S.; Musker, W. K. *J. Phys. Chem.* **1981**, *85*, 3767–3771. (d) Asmus, K.-D. In *Sulfur-centered Reactive Intermediates in Chemistry and Biology*; Chatgiliagoglu, C., Asmus, K.-D., Eds.; NATO ASI Series Vol. 197; Plenum: London, 1990; pp 155−172. (e) Glass, R. S. *Top. Curr. Chem.* **1999**, *205*, 1–87.

(37) Brunelle, P.; Rauk, A. *J. Phys. Chem. A.* **2004**, *108*, 11032–11041.

(38) Glass, R. S.; Petsom, A.; Hojjatie, M.; Coleman, B. R.; Duchek, J. R.; Klug, J.; Wilson, G. S. *J. Am. Chem. Soc.* **1988**, *110*, 4772–4778.

Scheme 1

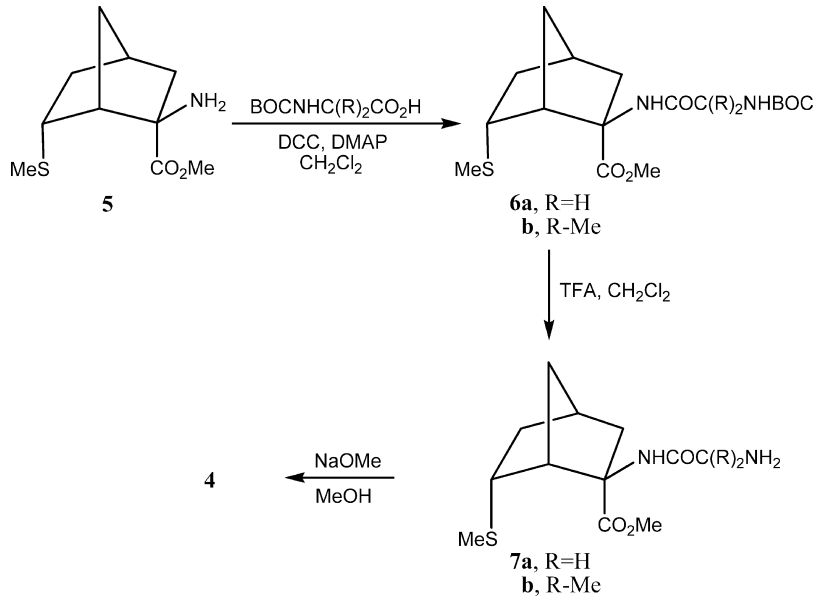

withdrawing α-amido substitution, as found in peptides, on neighboring amide participation.

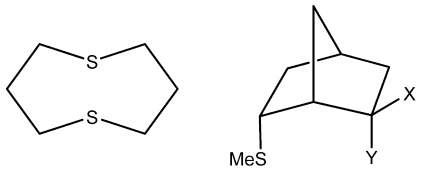

Results and Discussion

Synthesis. Compounds **2a** and **b** were synthesized as reported previously.[40] Compounds **3** and **4** were synthesized from the previously reported amino ester **5**.[41] Reaction of **5** with trimethylsilyl isocyanate followed by treatment of the crude product with sodium methoxide in methanol provided hydantoin **3** in 91% yield after column chromatography. 2,5-Diketopiperazines **4** were synthesized as shown in Scheme 1. All of the reactions shown in Scheme 1 proceeded quantitatively except for the coupling of **5** with BOC-dimethylglycine which occurred in 61% yield.

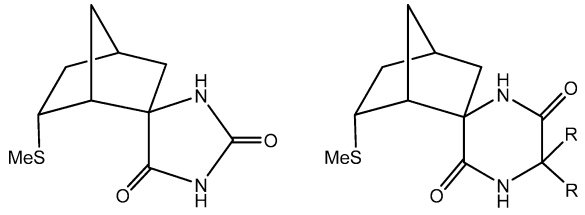

Amides **8a** and **b** were prepared as shown in Scheme 2. Diels−Alder reaction of amide **9a** or acid chloride **9b** (prepared from the known acid **9c**)[42] with 1,3-cyclopentadiene was unsuccessful even in the presence of lanthanide catalysts.[43] However, the following sequence proved successful in which

Scheme 2

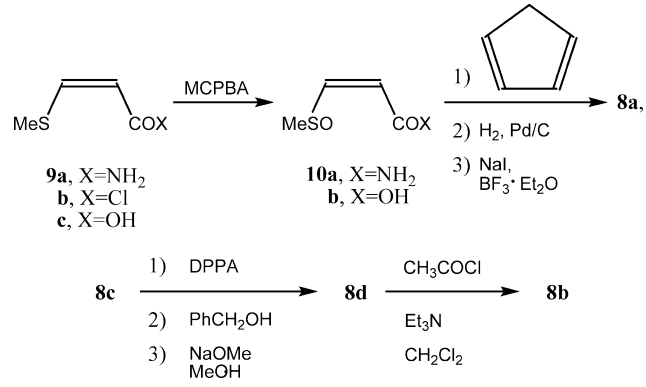

the corresponding sulfoxide acted as the dienophile.[44] Oxidation of **9a** with *m*-chloroperoxybenzoic acid (MCPBA) provided sulfoxide **10a** which was not isolated.

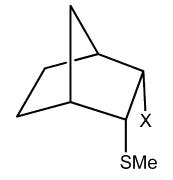

This crude product underwent Diels−Alder reaction with 1,3-cyclopentadiene overnight in an ice bath. Catalytic hydrogena-

(39) (a) Glass, R. S.; Hojjatie, M.; Wilson, G. S.; Mahling, S.; Göbl, M.; Asmus, K.-D. *J. Am. Chem. Soc.* **1984**, *106*, 5382–5383. (b) Asmus, K,-D.; Göbl, M.; Hiller, K.-O.; Mahling, S.; Mönig, J. *J. Chem. Soc. Perkin Trans. 2* **1985**, 641–646. (c) Mahling, S.; Asmus, K.-D.; Glass, R. S.; Hojjatie, M.; Sabahi, M.; Wilson, G. S. *J. Org. Chem.* **1987**, *52*, 3717–3724. (d) Steffen, L. K.; Glass, R. S.; Sabahi, M.; Wilson, G. S.; Schöneich, C.; Mahling, S.; Asmus, K.-D. *J. Am. Chem. Soc.* **1991**, *113*, 2141–2145.
(40) Glass, R. S.; Duchek, J. R.; Prabhu, U. D. G.; Setzer, W. N.; Wilson, G. S. *J. Org. Chem.* **1980**, *45*, 3640–3646.

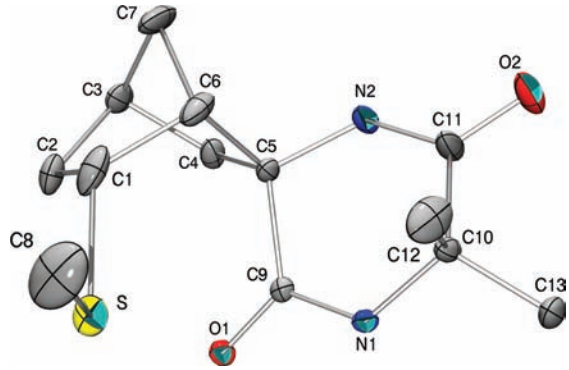

Figure 1. Drawing of **4b** derived from X-ray crystal structure study with displacement ellipsoids at 30% probability and hydrogen atoms omitted.

tion of this crude product followed by reduction of the sulfoxide with NaI and $BF_3 \cdot Et_2O$[45] afforded **8a**. The overall yield of pure **8a** in this sequence was 44%. Alternatively, Diels−Alder reaction of 1,3-cyclopentadiene with sulfoxide-carboxylic acid **10b**, obtained by MCPBA oxidation of **9c**, overnight in an ice bath followed by catalytic hydrogenation and NaI, $BF_3 \cdot Et_2O$ reduction, as outlined for the synthesis of **8a**, afforded carboxylic acid **8c** in 40% overall yield. Conversion of **8c** to amine **8d** was accomplished by a Curtius rearrangement. Heating **8a** with diphenylphosphoryl azide (DPPA)[46] followed by reaction with benzyl alcohol produced the rearranged carbamate, which on hydrolysis gave amine **8d**. Acetylation of this amine provided amide **8b**.

X-Ray Crystal Structure. A single crystal X-ray structure study of **4b** verified its molecular structure. A drawing of the molecule is shown in Figure 1 and an alternative view clarifying the orientation of the MeS- group relative to the diketopiperazine moiety is in the Supporting Information. The crystal data, bond length, bond angles and torsion angles are given in the Supporting Information. In the crystal structure of **4b**, the S···O distance is approximately 3.0 Å (there is some disorder in the SMe group) rendering it within the range in which there may be nonbonded interactions. Such interactions have been analyzed previously.[47] The 1,4-diketopiperazine moiety in **4b** adopts a typical boat conformation in the solid state.[48]

Electrochemistry. Comparison of **3**, **4a** and **b** with **2a**, **8a** and **b** reveals two important structural differences relevant to neighboring group participation on oxidation. The first is that an electron-withdrawing amide group is appended α- to the participating amide group. Such a substitution should disfavor participation electronically but such an arrangement is more analogous to peptide backbone amides. In addition, geometric constraints permit participation by the amide oxygen but preclude participation by the amide nitrogen. Formation of S−N bonded species on oxidation of peptides and proteins has been reported.[29c,49]

Table 1. Peak Potentials (E_p) for the Oxidation of **2a**, **b**, **3**, **4a**, **b**, **8a** and **b**

cmpd	E_p[a], V
2a	1.07
2b	1.40[b]
3	1.16
4a	1.11
4b	1.08
8a	0.99
8b	1.25

[a] Peak potentials for oxidation determined at a Pt electrode (2 mm diam), 0.1 V/s scan rate and measured in acetonitrile, 0.1 M n-Bu_4NClO_4 vs Ag/0.1 M $AgNO_3$ in acetonitrile reference electrode. [b] From ref 38.

The oxidation of **3**, **4a** and **b**, and **8a** and **b** were studied electrochemically in acetonitrile using the technique of cyclic voltammetry under conditions comparable to those used for amides **2a** and **b** reported previously.[38] All of the compounds undergo irreversible oxidation. The observed peak potentials are listed in Table 1. Because the previously reported peak potential for **2a** was substantially less anodic than the other compounds studied, it was reinvestigated. The peak potential for **2a** was redetermined to be 1.07 V. The difference between the previous value and the redetermined value is ascribed to redox catalysis by Br^-. It has been reported[38] that trace amounts of Br^- in the supporting electrolyte lowers the oxidation potential of **2**, X = H, Y = CO_2^-; **2**, X = H, Y = CH_2OH and **2**, X = H, Y = CMe_2OH. The supporting electrolyte currently used (n-Bu_4NPF_6) is known to be Br^- free and bromide free sodium perchlorate showed the same results as those with n-Bu_4NPF_6. Consequently, LiBr was added to a solution of **2a** in acetonitrile/0.1 M n-Bu_4NPF_6. A new oxidation peak was observed at a peak potential of 0.83 V in the presence of 0.7 mM LiBr. It would be reasonable to conclude that the previously reported value for the oxidation of **2a** was due to the presence of Br^- in the supporting electrolyte and the value of 1.07 V is the potential in the absence of Br^-. The Br^- redox catalysis may be relevant to two-electron oxidation coupled with atom transfer of methionine in proteins.[50] There have been studies on the oxidation of methionine residues in proteins by hydrogen peroxide.[7−9,51] The mechanism for the reaction involves a two-electron oxidation of sulfur coupled with oxygen transfer.[52] The rates of such oxidations for the proteins studied have been interpreted in terms of two shell water coordination number[51] with little effect ascribed to potential neighboring groups. However, oxidation of Met(1) in rhG-CSF by hydrogen peroxide showed an anomalously low activation energy.[7a] Although this was ascribed to the negative charge on the C-terminus, it may be an example of neighboring carboxylate participation in two-electron transfer coupled with atom transfer oxidation of sulfur. In this regard, the results on redox catalysis are pertinent. Studies on electrochemical

(41) Glass, R. S.; Hojjatie, M.; Sabahi, M.; Steffen, L. K. *J. Org. Chem.* **1990**, *55*, 3797–3804.
(42) De Medeiros, E. F.; Herbert, J. M.; Taylor, R. J. K. *J. Chem. Soc., Perkin Trans. 1* **1991**, 2725–2730.
(43) (a) Kobayashi, S.; Hachiya, I.; Takahori, T.; Araki, M.; Ishitani, H. *Tetrahedron Lett.* **1992**, *33*, 6815–6818. (b) Libing, Y.; Chen, D.; Wang, P. G. *Tetrahedron Lett.* **1996**, *37*, 2169–2172.
(44) Ordóñez, M.; de la Rosa, V. G.; Alcudia, F.; Llera, J. M. *Tetrahedron* **2004**, *60*, 871–875.
(45) (a) Vankur, Y. D.; Rao, C. T. *Tetrahedron Lett.* **1985**, *26*, 2717–2720. (b) García Ruano, J. L.; Martín Castro, A. M.; Rodríguez Ramos, J. H.; Rubio Flamarique, A. C. *Tetrahedron Asym.* **1997**, *8*, 3503–3511.
(46) (a) Shioiri, T.; Ninomiya, K.; Yamada, S. *J. Am. Chem. Soc.* **1972**, *94*, 6203–6205. (b) Ninomiya, K.; Shioiri, T.; Yamada, S. *Tetrahedron* **1974**, *30*, 2151–2157.
(47) Iwaoka, M.; Takemoto, S.; Tomoda, S. *J. Am. Chem. Soc.* **2002**, *124*, 10613–10620.
(48) (a) Zhu, Y.; Tang, M.; Shi, X.; Zhao, Y. *Int. J. Quantum Chem.* **2007**, *107*, 745–753. (b) Bettens, F. L.; Bettens, R. P. A.; Brown, R. D.; Godfrey, P. D. *J. Am. Chem. Soc.* **2000**, *122*, 5856–5860.
(49) Nauser, T.; Jacoby, M.; Koppenol, W. H.; Squier, T. C.; Schöneich, C. *Chem. Commun.* **2005**, 587–589.
(50) Glass, R. S. In *Sulfur-centered Reactive Intermediates in Chemistry and Biology*; Chatgilialoglu, C., Asmus, K.-D., Eds.; NATO ASI Series, Vol. 197; Plenum: London, 1990; pp 213−226. Glass, R. S. *Rev. Heteroatom Chem.* **1996**, *15*, 1–24.
(51) Chu, J.-W.; Brooks, B. R.; Trout, B. L. *J. Am. Chem. Soc.* **2004**, *126*, 16601–16607.
(52) Chu, J.-W.; Trout, B. L. *J. Am. Chem. Soc.* **2004**, *126*, 900–908.

oxidation of **2c** showed Br^- redox catalysis[53] in which oxidation of Br^- forms Br_2.[54] The oxidation of **2c** by Br_2, which is a two-electron oxidation coupled with Br transfer, is facilitated by neighboring carboxylate participation. Consequently, redox catalysis by Br^- resulting in the oxidation of **2a** suggests that amide group participation in two-electron oxidation coupled with atom transfer of methionine residues in proteins may also affect the rate of such oxidations in suitable cases, that is, those in which the thioether sulfur and amide moieties are juxtaposed.

The oxidation peak potential for **2a** in the absence of Br^- is more in accord with those of **3**, **4a** and **b**, **8a** and **b** shown in Table 1. This oxidation potential for **2a** is still 350 mV less anodic than that for **2b** (which is unaffected by Br^-). The substantially less anodic peak potentials for endoamides **2a**, **8a** and **b** illustrate the facilitated oxidation owing to neighboring amide participation. Such participation is possible for **2a**, **8a** and **b** but is geometrically precluded for **2b**. This facilitation could be due to S−O or S−N bond formation in **2a** or **8a**. However, S−N bond formation is unfavorable in **8b** because it results in a strained 4-membered ring; whereas S−O bond formation results in a 6-membered ring. It is also worth noting that either S−O or S−N bond formation in **8a** result in a 5-membered ring; whereas S−O or S−N bond formation in **2a** results in a 6-membered ring.

The electrochemistry of **3** was studied in more detail. Controlled potential coulometry of **3** with the potential set at +1.4 V resulted in the transfer of two electrons per molecule. Varying the scan rate from 0.1 to 10 V/s in cyclic voltammetric experiments with **3** resulted in increasing anodic current with increasing scan rate with the expected positive shift in E_p with increasing scan rate. Plots of the oxidation peak currents versus $v^{1/2}$ and v indicate that there is diffusion rather than adsorption control, but also that adsorption control appears to become rate limiting at high scan rates.

In the oxidation of **3**, **4a** and **b** only S−O bond formation is possible, owing to the spiro fusion in these compounds. However, as pointed out above, an electron-withdrawing amide moiety disfavors participation. In comparing the oxidation potentials of **3**, **4a** and **b** with **2b**, it is clear that there is facilitated oxidation for these compounds. However, comparison with **2a** suggests that the electron-withdrawing amide group mitigates this effect. In comparing **8a**, in which participation results in a 5-membered ring, with **2a** and **8b**, in which participation results in a 6-membered ring, formation of a 5-membered ring appears to result in a greater lowering of the oxidation potential compared with forming a 6-membered ring.

The facilitation of thioether oxidation owing to S−O bond formation with a neighboring amide contrasts with the theoretical calculations suggesting that methionine in peptide environments would not undergo a lowering of $E°$ despite 2c-3e S∴O bond formation.[37] Although we measured E_p and not $E°$, the two measures typically track each other.[34,55] However, the calculations were done for one-electron oxidation in water whereas our electrochemical studies were done in acetonitrile. Solvent effects on one-electron oxidation potentials of thioethers are known[55] and depend mainly on solvent dipolarity/polarizability (π^* in the Kamlet−Taft relationship). Whether the solvent differences can affect the neighboring amide effect on oxidation potentials is unclear. Whether water or acetonitrile is a better model for the environment of methionine in β-amyloid peptide oligomers is also not clear. Amyloid assemblies feature steric zippers of cross-β spines which exclude water.[56] Aβ(1−42) Fibrils undergo slow exchange in the 18−42 residue region suggesting solvent inaccessibility in this region.[57] The positioning of the methionine side chain in these aggregates is unknown but photoaffinity cross-linking of Aβ(1−40) F4Bpa suggests interchain proximity of the Met(35) side chain and Phe(4) resulting from an antiparallel alignment of Aβ peptides.[58] The conclusion is that amide oxygen participation indeed lowers the oxidation potential of sulfides even in compounds appended with α-amido groups.

Pulse Radiolysis. Amide oxygen participation in the oxidation of sulfides requires that an S−O bond is formed. To provide evidence that this indeed occurs, these compounds were studied using the technique of pulse radiolysis.

Radiation chemical processes and yields of primary radicals. The irradiation of water yields hydrated electrons (e_{aq}^-), H• atoms, and hydroxyl radicals (HO•), where hydrated electrons are converted into hydroxyl radicals through reaction with N_2O (reactions 1 and 2).[59]

$$H_2O \rightarrow e_{aq}^-, H^\bullet, HO^\bullet \quad (1)$$

$$e_{aq}^- + H_2O + N_2O \rightarrow HO^\bullet + HO^- + N_2 \quad (2)$$

In N_2O-saturated solution, the initial yield of hydroxyl radicals, $G(HO^\bullet)_i$, available for the reaction with a substrate S is calculated using eq 3,[60] where k_S represents the rate constant for the reaction of HO• with the substrate S.

$$G(HO^\bullet)_i = 5.2 + 3.0\frac{[k_s[S]/(4.7\times10^8)]^{1/2}}{1 + [k_s[S]/(4.7\times10^8)]^{1/2}} \quad (3)$$

On the basis of the rate constant for the reaction of HO• with methionine,[61] we assume $k_S = 1 \times 10^{10}\ M^{-1}s^{-1}$ for the reaction of HO• with the norbornyl derivatives under investigation, and for the applied concentrations of norbornyl derivatives used: 0.2 mM, we calculate $G(HO^\bullet)_i = 5.35$ ($G = 1.0$ corresponds to 0.1036 μmol/J).

The one-electron oxidation of substrate by HO• yields substrate radical cation, $S^{+\bullet}$, and HO^-, which in acidic solution is immediately neutralized with H^+ (reaction 4). Hence, reaction 4

$$HO^\bullet + S + H^+ \rightarrow H_2O + S^{+\bullet} \quad (4)$$

(53) Glass, R. S.; Petsom, A.; Hojjatie, M.; Coleman, B. R.; Duchek, J. R.; Klug, J.; Wilson, G. S. *J. Am. Chem. Soc.* **1988**, *110*, 4772–4778.
(54) An alternative mechanism may involve reaction of Br˙ with **2c** to form a 2c-3e Br-S species:Hiller, K.-O.; Asmus, K.-D. *Int. J. Radiat. Biol.* **1981**, *40*, 583–595.
(55) Taras-Goslinska, K.; Jonsson, M. *J. Phys. Chem. A* **2006**, *110*, 9513–9517.
(56) Eisenberg, D.; Nelson, R.; Sawaya, M. R.; Balbirnie, M.; Sambashivan, S.; Ivanova, M. I.; Madsen, A. O.; Riekel, C. *Acc. Chem. Res.* **2006**, *39*, 568–575. Teplow, D. B.; Lazo, N. D.; Bitan, G.; Bernstein, S.; Wyttenbach, T.; Bowers, M. T.; Baumketner, A.; Shea, J.-E.; Urbanc, B.; Cruz, L.; Borreguero, J.; Stanley, H. E. *Acc. Chem. Res.* **2006**, *39*, 635–645. Sawaya, M. R.; Sambashivan, S.; Nelson, R.; Ivanova, M. I.; Sievers, S. A.; Apostol, M. I.; Thompson, M. J.; Balbirnie, M.; Wiltzius, J. J. W.; McFarlane, H. T.; Madsen, A. O.; Riekel, C.; Eisenberg, D. *Nature* **2007**, *447*, 453–456.
(57) Lührs, T.; Ritter, C.; Adrian, M.; Rick-Loher, D.; Bohrmann, B.; Döbeli, H.; Schubert, D.; Riek, R. *Proc. Natl. Acad. Sci. U.S.A.* **2005**, *102*, 17342–17347.
(58) Egnaczyk, G. F.; Greis, K. D.; Stimson, E. R.; Maggio, J. E. *Biochemistry* **2001**, *40*, 11706–11714.
(59) Von Sonntag, C. *The Chemical Basis of Radiation Biology*; Taylor & Francis: London, 1987.
(60) Schuler, R. H.; Hartzell, A. L.; Behar, B. *J. Phys. Chem.* **1981**, *85*, 192–199.
(61) Buxton, G. V.; Greenstock, C. L.; Helman, W. P.; Ross, A. B. *J. Phys. Chem. Ref. Data* **1988**, *17*, 513–886.

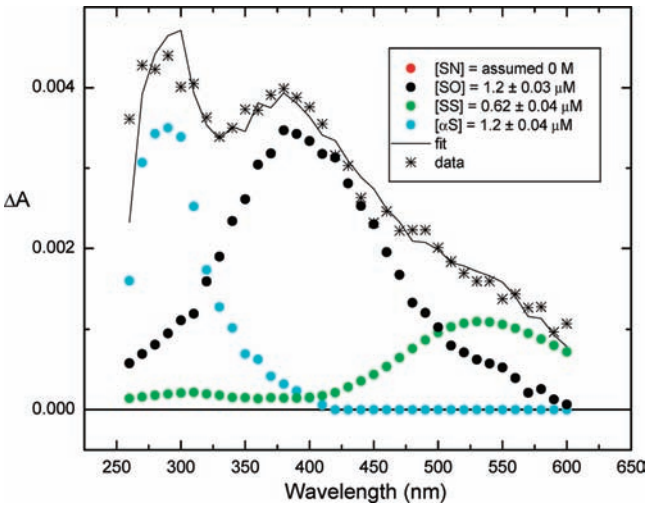

Figure 2. Experimental spectrum (*) of 0.2 mM **2a** at pH 4 in N_2O-saturated aqueous solution 4 μs after pulse irradiation and fit using $\varepsilon(SS^+) = 1776\ M^{-1}\ cm^{-1}$, SO taken from ref 83 but λ_{max} blue-shifted by 20 nm to 380 nm and SS^+ derived from **4b** and αS derived from **2b**.

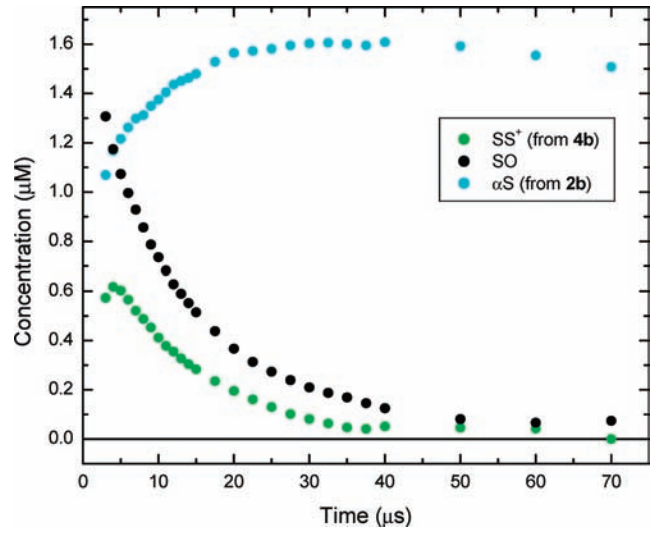

Figure 3. Quantification of the concentration changes for 0.2 mM **2a** at pH 4 after pulse irradiation (dosimetry $[(SCN)_2^-] = 3.47\ \mu M$ in $[SCN^-] = 0.1$ M N_2O saturated solution).

leads to the replacement of highly conducting protons ($\Lambda_0 = 315$ S cm^2 eq^{-1})[62] with less conducting substrate radical cations ($\Lambda_0 \approx 45$ S cm^2 eq^{-1}),[39d] resulting in a loss of conductivity. Therefore, the reaction of HO$^\bullet$ with the norbornyl derivatives has been monitored by both time-resolved absorption spectroscopy and time-resolved conductivity measurements.

Oxidation of 2a and 2b. Figure 2 displays the experimental spectrum (symbol *) recorded at 4 μs after pulse irradiation of an N_2O-saturated aqueous solution, pH 4, containing 0.2 mM **2a**. The applied dose was $D = 4.8$ Gy, which translates into initial concentrations of $[HO^\bullet]_i = 2.65 \times 10^{-6}$ M and $[H^\bullet]_i = 0.3 \times 10^{-6}$ M. The experimental spectrum is characterized by

Scheme 3

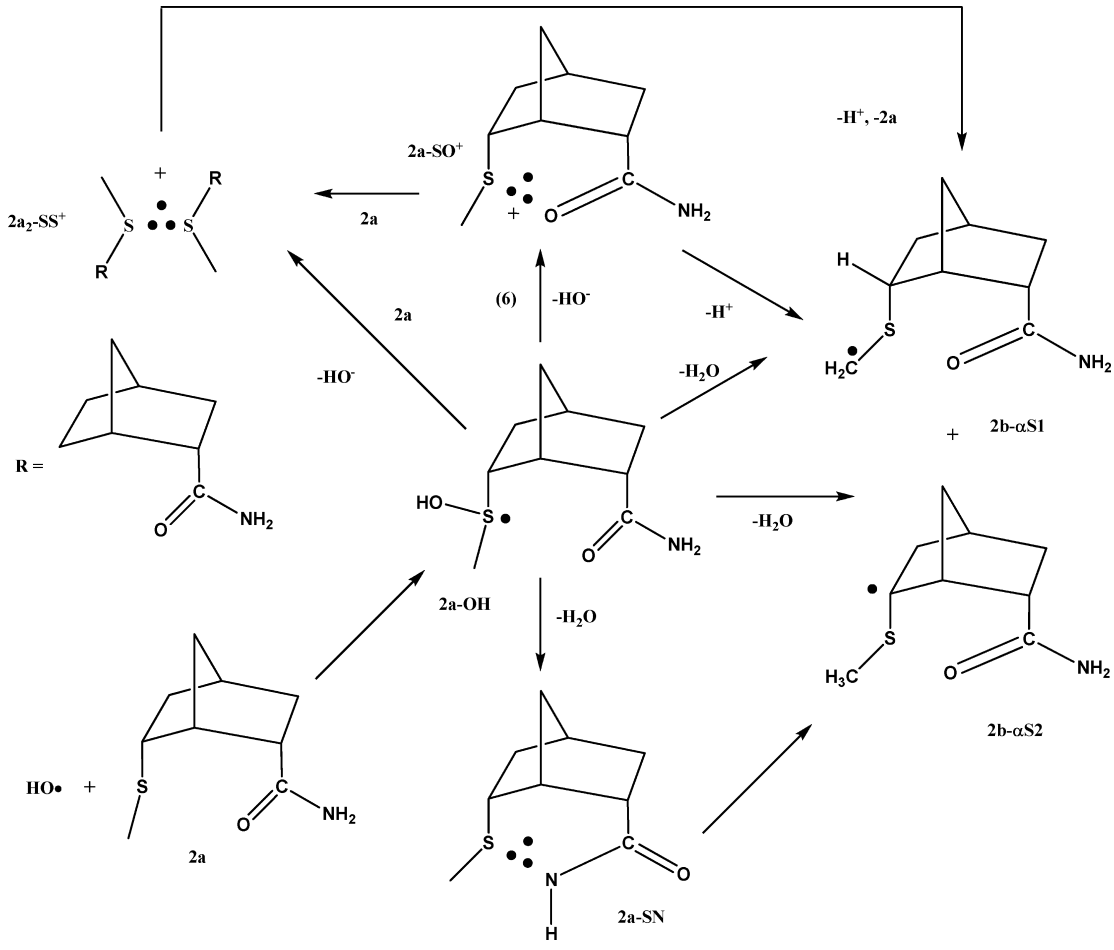

Scheme 4

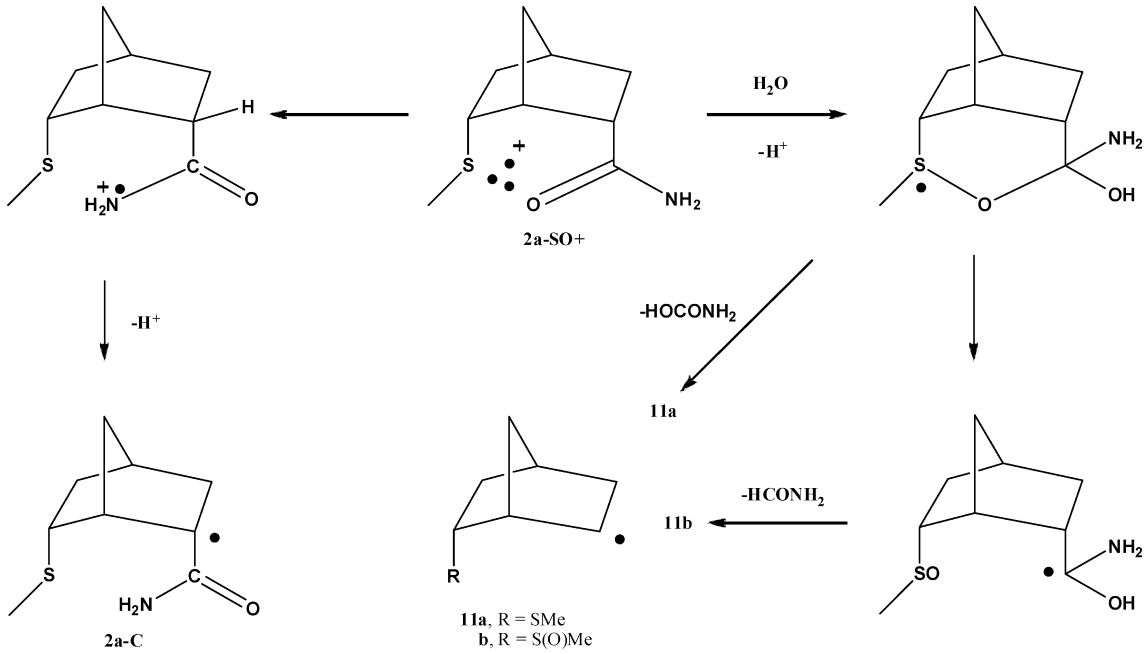

two absorbance maxima around 285 and 380 nm, generated through the oxidation of **2a** by HO$^{\bullet}$.

Scheme 3 summarizes the expected reactions of HO$^{\bullet}$ with **2a**, based on analogous processes with Met-containing peptides.[29a,c] Addition of HO$^{\bullet}$ to the thioether moiety of **2a** yields the short-lived hydroxysulfuranyl radical **2a-OH**, which decomposes into sulfur radical cation or neutral radical complexes such as the sulfur−oxygen bonded radical cation **2a-SO**$^+$, or the sulfur−sulfur bonded dimeric radical cation **2a$_2$-SS**$^+$, or the sulfur−nitrogen bonded radical **2a-SN**. Ultimately, these sulfur radicals convert into the carbon-centered radicals **2a-αS1** and/or **2a-αS2**. All these intermediates will show distinct absorption spectra, and reference spectra for these individual intermediates have been recorded. A deconvolution procedure to fit the experimental spectra with these reference spectra of the individual intermediates displayed in Scheme 3 has been described in detail elsewhere.[63] This procedure was applied to the spectrum in Figure 2, using the following reference spectra: for **2a-OH**,[29a] $\lambda_{max} = 340$ nm and $\epsilon_{340} = 3400$ M^{-1} cm^{-1}, **2a-SN**,[29a,c] $\lambda_{max} = 390$ nm and $\epsilon_{390} = 4500$ M^{-1} cm^{-1}, for **2a$_2$-SS**$^+$, $\lambda_{max} = 525$ and $\epsilon_{525} = 1776$ M^{-1} cm^{-1} (this work, see below), for **2a-αS1** and **2a-αS2**, $\lambda_{max} = 285$ nm (this work, see below) and $\epsilon_{285} = 3000$ M^{-1} cm^{-1},[64] for **2a-SO**$^+$,[65] $\lambda_{max} = 390$ nm and $\epsilon_{390} = 3{,}125$ M^{-1} cm^{-1}.

A best fit of the experimental spectrum, represented by the solid line, was obtained with the individual components shown in Figure 2. Importantly, the deconvolution indicates that the hydroxysulfuranyl radical **2a-OH** decomposes into **2a-SS**$^+$, **2a-SO**$^+$, and **2a-αS1/2a-αS2**, but not the sulfur−nitrogen bonded radical cation **2a-SN**$^+$. Taking the known extinction coefficients of **2a-SO**$^+$, **2a$_2$-SS**$^+$, and **2a-αS1/2a-αS2**, we calculate a total concentration of intermediates of 3.02 μM at 4 μs after the pulse, in excellent agreement with the combined initial yields of $[HO^{\bullet}]_i = 2.65$ μM and $[H^{\bullet}]_i = 0.3$ μM, that is, $[HO^{\bullet}]_i + [H^{\bullet}]_i = 2.95$ μM. Here, the H$^{\bullet}$ atom will react predominantly with the thioether moiety, likely directly leading to **2a-αS1/2a-αS2**, though a fraction could also cause homolytic C−S bond cleavage.[66]

Parallel conductivity experiments reveal that at 4 μs after the pulse irradiation of **2a**, $G \times \Lambda_0 = -103.6 \times 10^{-6}$ S cm^2 J^{-1}, corresponding to the replacement of ca. 1.83 μM protons by ca. 1.83 μM sulfur-radical cations according to the general reaction 4. This concentration agrees well with the combined yield of the radical cations **2a-SS**$^+$ and **2a-SO**$^+$, 1.82 μM, quantified in Figure 2. Several control deconvolution experiments have been performed. The deconvolution of the spectrum displayed in Figure S1 (Supporting Information) was achieved by replacing the sulfur−oxygen bonded radical cations by the sulfur−nitrogen bond. The total yield of reactive intermediates amounts to 2.7 μM at 4 μs after the pulse, that is, slightly lower compared to $[HO^{\bullet}]_i + [H^{\bullet}]_i$. However, most importantly the deconvolution in Figure S1 would require the intermediate **2a-SN** to exist as radical cation, that is, in its protonated form, **2a-SN**$^+$. This disagrees with several earlier experiments, which have shown that formation of such sulfur−nitrogen bonded intermediates occurs with nitrogen deprotonation, that is, the formation of neutral species, even at pH 4.[67] Therefore we would eliminate **2a-SN**$^+$ as a contributor to our experimental spectrum.

Figure 3 shows concentration vs time profiles for **2a$_2$-SS**$^+$, **2a-SO**$^+$ and **2a-αS1/2a-αS2**. Two important features must be noted: (i) all the radical cation species fully decompose within ca. 50 μs after the pulse; (ii) the combined yield of **2a$_2$-SS**$^+$ and **2a-SO**$^+$, 1.82 μM (at 4 μs after the pulse), does not convert solely into **2a-αS1/2a-αS2**, which only increases by ca. 0.4 μM between 4 and 50 μs after the pulse (some second-order radical−radical reactions may occur but they probably cannot account for the entire discrepancy). Hence, other decomposition

(62) Asmus, K.-D. *Int. J. Radiat. Phys. Chem.* **1972**, *4*, 417–437. (b) *Landolt-Börnstein Zahlenwerte und Funktionen, Vol. 7 II*; Springer Verlag: Berlin, 1960.
(63) Marciniak, B.; Bobrowski, K.; Hug, G. L. *J. Phys. Chem.* **1993**, *97*, 11937–11943.
(64) Hiller, K.-O.; Asmus, K.-D. *Int. J. Radiat. Biol.* **1981**, *40*, 597–604.
(65) Schöneich, C.; Zhao, F.; Madden, K. P.; Bobrowski, K. *J. Am. Chem. Soc.* **1994**, *116*, 4641–4652.
(66) Mozziconacci, O.; Bobrowski, K.; Ferreri, C.; Chatgilialoglu, C. *Chemistry* **2007**, *13*, 2029–2033.
(67) Bobrowski, K.; Hug, G. L.; Pogocki, D.; Marciniak, B.; Schöneich, C. *J. Phys. Chem. B* **2007**, *111*, 9608–9620.

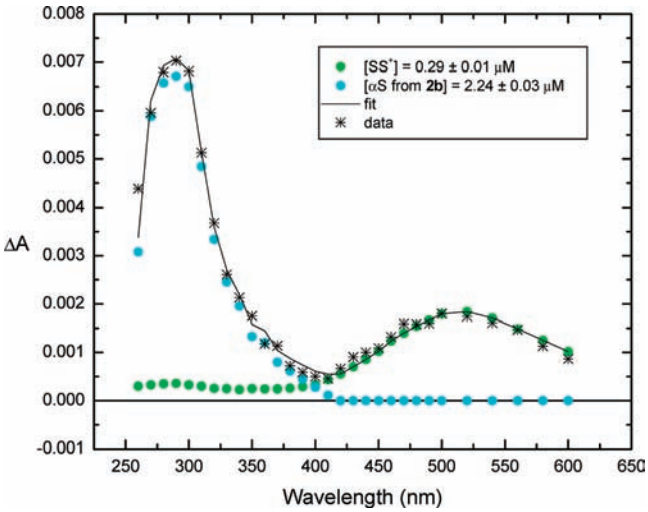

Figure 4. Experimental spectrum (*) of 0.2 mM **2b** at pH 4 in N_2O-saturated aqueous solution 4 μs after pulse irradiation and fit using $\varepsilon_{520}(SS^+) = 1776\ M^{-1}\ cm^{-1}$, $[OH]_i = 3.43\ \mu M$.

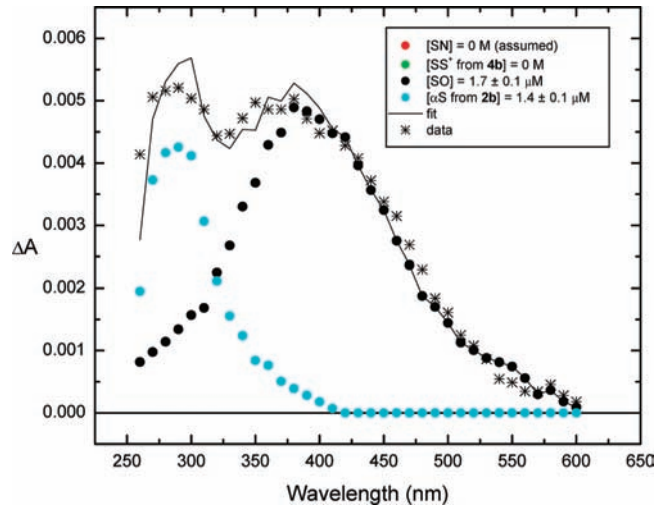

Figure 5. Experimental spectrum (*) of 0.2 mM **8a** at pH 4 in N_2O-saturated aqueous solution 4 μs after pulse irradiation and fit using $\varepsilon_{530}(SS^+) = 1776\ M^{-1}\ cm^{-1}$, $[OH]_i = 3.4\ \mu M$.

pathways must be available, and some proposed reactions are outlined in Scheme 4.

Figure 4 displays the absorption spectrum recorded at 4 μs after pulse irradiation of an N_2O-saturated aqueous solution, pH 4, containing 0.2 mM **2b**. It is characterized by two peaks with $\lambda_{max} = 285$ and 525 nm. The rigid geometry of **2b** precludes the formation of sulfur−oxygen or sulfur−nitrogen bonded radical cations. Thus **2b$_2$-SS$^+$** and **2b-αS1/2b-αS2** are the only intermediates, which can arise from the initial hydroxysulfuranyl radical **2b−OH** Scheme 5.

The combined yield of **2b$_2$-SS$^+$** and **2b-αS1/2b-αS2** amounts to 2.53 μM at 4 μs after the pulse, which is about 34% too low (relative to the initial yields of HO$^\bullet$ and H$^\bullet$) and may reflect slightly different extinction coefficients for the radical intermediates from **2a** and **2b**. However, importantly the experimental spectrum in Figure 4 (symbol *) can be fitted well with only contributions from **2b$_2$-SS$^+$** and **2b-αS1/2b-αS2**. A similar picture is obtained for pulse irradiation of **2b** at pH 5 (data not shown). Because of the clear separation of the 285 nm band from the 525 nm band, the 285 nm band from **2b** was taken as a reference spectrum for all α-(alkylthio)alkyl radicals obtained from the norbornyl systems under investigation.

Oxidation of 8a and 8b. Figure 5 displays the optical spectra recorded at 4 μs after pulse irradiation of an N_2O-saturated aqueous solution, pH 4, containing 0.2 mM **8a**. The applied dose was $D = 6.2$ Gy, which translates into initial concentrations of $[HO^\bullet]_i = 3.4 \times 10^{-6}$ M and $[H^\bullet]_i = 0.4 \times 10^{-6}$ M. The experimental spectrum (symbol *) is deconvoluted into contributions from **8a-SO$^+$** (with $\lambda_{max} = 390$ nm) and from **8a-αS1/8a-αS2** (Scheme 6). The overall yield of intermediates is calculated to be 3.1 μM, which accounts

Scheme 5

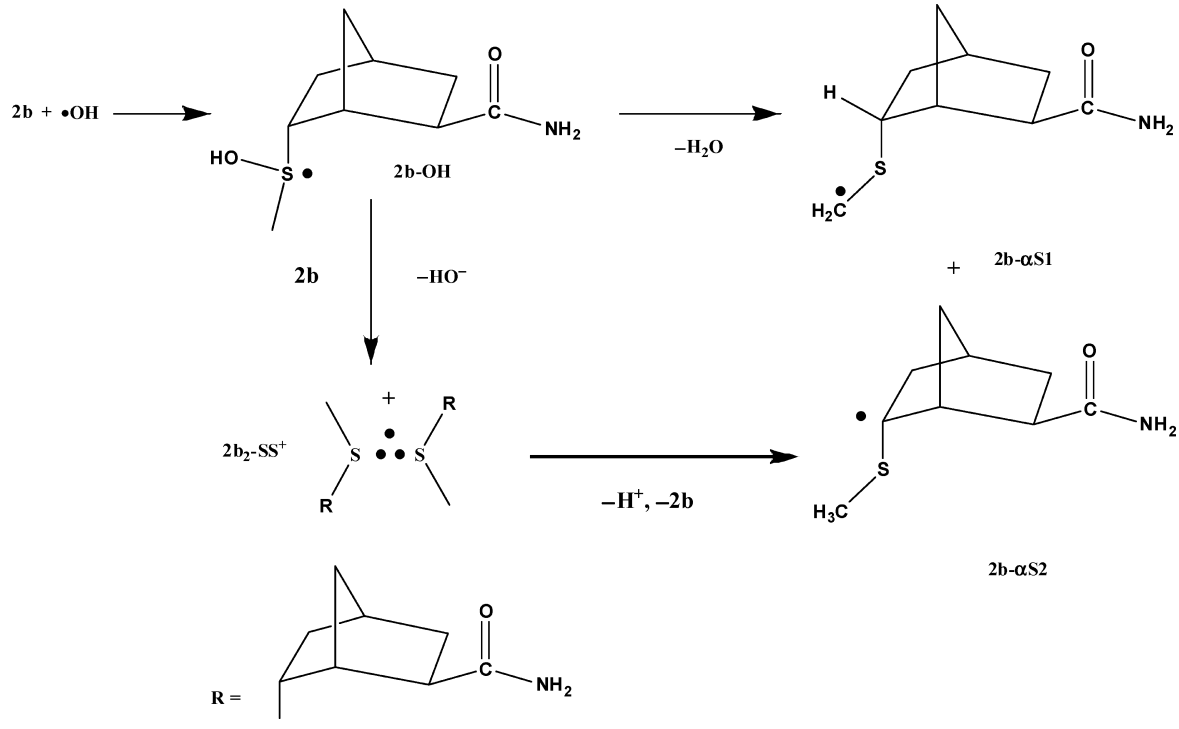

Scheme 6

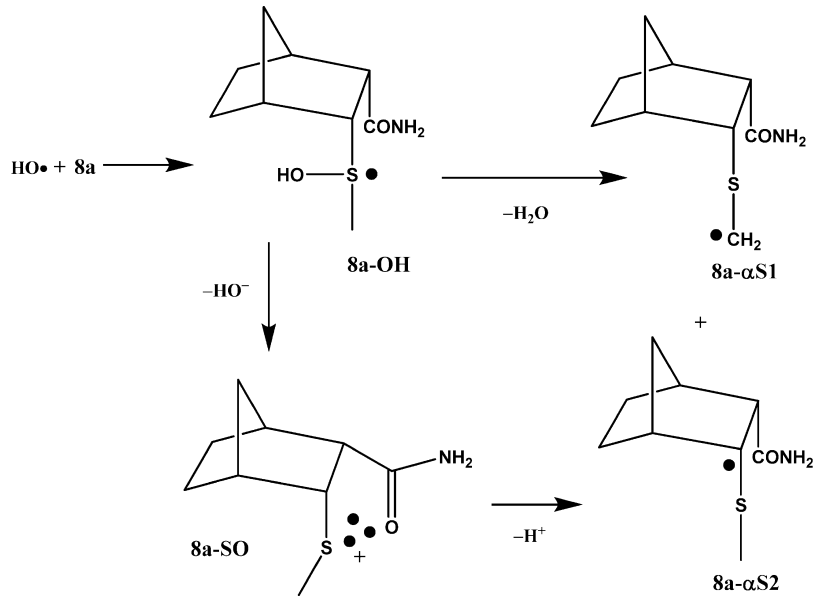

for 82% of the initial yield of $[HO^{\bullet}]_i + [H^{\bullet}]_i = 3.8\ \mu M$. Parallel conductivity measurements reveal that at 4 μs after the pulse, $G \times \Lambda_0 = -84.5 \times 10^{-6}$ S cm^2 J^{-1}, corresponding to a yield of radical ions (via the general reaction 4) of 1.94 μM. This value agrees reasonably well with the yield of **8a-SO**$^+$, 1.7 $\pm$ 0.1 μM. Importantly, the sulfur−oxygen bonded radical cation **8a-SO**$^+$ is rather stable, with only about 20% decomposition over a time period of 50 μs as seen in Figure 6 (compared to a complete decomposition of **2a-SO**$^+$ within 50 μs; Figure 3). Similar results were observed at pH 5 (data not shown).

Interestingly, the pulse irradiation of an N_2O-saturated aqueous solution at pH 4, containing 0.2 mM **8b** yields a completely different picture. Here, the α-(alkylthio)alkyl radicals **8b-αS1/8b-αS2** (Scheme 7) are the only species present at 4 μs after the pulse (Figure 7). Only for 1−2 μs after the pulse do we observe an absorption in the 390 nm region, which can be ascribed to either a very short-lived sulfur−nitrogen or sulfur−oxygen bonded radical/radical cation (these intermediates have not been included in Scheme 7).

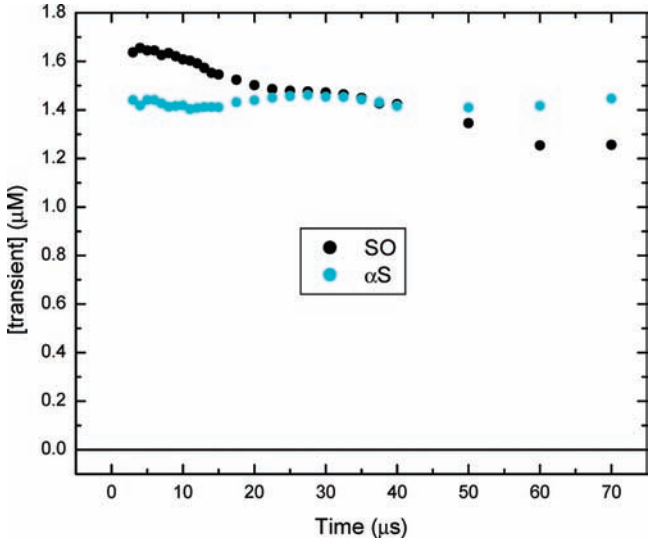

Figure 6. Quantification of the concentration changes for 0.2 mM **8a** at pH 4 after pulse irradiation $[OH]_i = 3.4\ \mu M$.

Oxidation of Diketopiperazine 4a. In diketopiperazine **4a**, only O can intramolecularly interact with a sulfide radical cation owing to molecular constraints and such interaction results in the formation of the sulfur−oxygen bonded intermediate **4a-SO**$^+$. Pulse irradiation of an N_2O-saturated aqueous solution, pH 5, containing 0.2 mM **4a** leads to the absorbance spectra shown in Figure 8. The experimental spectra can be deconvoluted into contributions from **4a-αS1/4a-αS2**, **4a$_2$-SS**$^+$ and diketopiperazyl radical **4a-C**$^{\bullet}$ (with λ_{max} = 265 and 365 nm and extinction coefficients of 8500 and 2500 M^{-1}cm^{-1}, respectively)[68] as illustrated in Figure 9 for 1.2 μs after the pulse. As seen in the figure, this accounts well for the experimental spectrum except for a relatively sharp band with λ_{max} = 390 nm. This feature is assigned to **4a-SO**$^+$ but it is considerably sharper than the previously observed SO^+ species. This sharpness may be a consequence of its constrained framework, an aspect which will be investigated further in the future. The overall reactions are summarized in Scheme 8. The low yield of diketopiperazyl radical **4a-C**$^{\bullet}$ is expected since the rate constant for the reaction of diketopiperazine itself with HO$^{\bullet}$ radicals,[69] 1×10^9 M^{-1} s^{-1}, is *ca.* an order of magnitude lower compared to the rate constant for reaction of HO$^{\bullet}$ with thioethers. Importantly, while the sulfur−oxygen bonded species **4a-SO**$^+$ decomposes even over short time scales, no additional absorbance at 285 nm is built up, suggesting that **4a-SO**$^+$ decomposes via alternative routes, which do not yield **4a-αS1/4a-αS2**. A comparable feature was observed for radical cations of **2a**, which were not exclusively converted into **2a-αS1/2a-αS2** (see above). Scheme 9 summarizes a series of potential reactions by which **4a-SO**$^+$ may decompose. N−H deprotonation of **4a-SO**$^+$ as shown in the first hypothesized reaction may be facile. Oxygen transfer, shown in the second reaction, would be driven by sulfoxide stabilization and by nitrogen stabilization of the resulting radical cation. The last reaction involves an electron-transfer decarbonylation which is analogous to the known[39d] decarboxylation of the amino acid corresponding to amino ester **5** on pulse radiolysis.

The low yield of sulfur−sulfur bonded dimeric radical cation is surprising, and in order to test whether such species would be stable under appropriate experimental conditions,

(68) Hayon, E.; Simic, M. *J. Am. Chem. Soc.* **1971**, *93*, 6781–6786.
(69) Mieden, O. J.; von Sonntag, C. *Z. Naturforsch.* **1989**, *44b*, 959–974.

Scheme 7

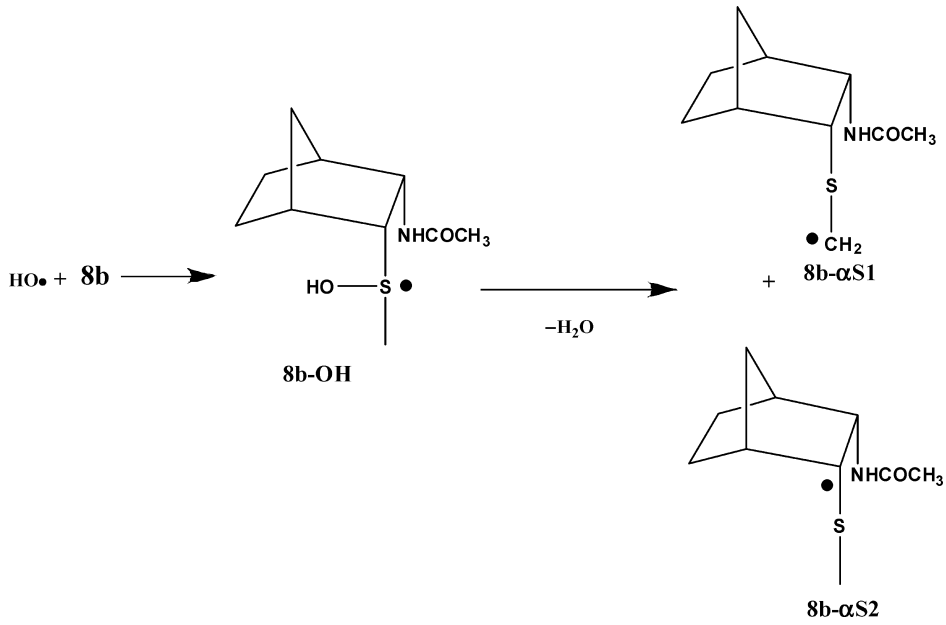

we reverted to an alternate route of radical cation generation through oxidation of **4a** by the sulfate radical anion, $SO_4^{-\bullet}$. The pulse irradiation of an Ar-saturated aqueous solution, pH 4, containing 5 mM $K_2S_2O_8$, 3 M *tert.*-butyl alcohol, and 4 mM **4a** resulted in the optical spectrum displayed in Figure 10. The spectrum shows an absorption maximum with λ_{max} = 525 nm, which is characteristic for sulfur−sulfur bonded radical cations. Under the applied experimental conditions, this species is formed selectively from $SO_4^{-\bullet}$ as shown in reactions 5−7.

$$e_{aq}^- + S_2O_8^{2-} \rightarrow SO_4^{2-} + SO_4^{\bullet-} \quad (5)$$

$$HO^\bullet + \textit{tert}\text{-butyl alcohol} \rightarrow H_2O + {}^\bullet CH_2C(CH_3)_2OH \quad (6)$$

$$SO_4^{-\bullet} + 2\,\mathbf{4a} \rightarrow SO_4^{2-} + \mathbf{4a}^{+\bullet}(+\mathbf{4a}) \rightarrow \mathbf{4a_2\text{-}SS}^+ \quad (7)$$

Based on the radiation chemical yield $SO_4^{-\bullet}$ and on a complete reaction of $SO_4^{-\bullet}$ with **4a**, we calculate an extinction coefficient for $\mathbf{4a_2\text{-}SS}^+$ of ϵ_{525} = 1,776 M^{-1} cm^{-1}. Though on the lower end of extinction coefficients reported for sulfur−sulfur bonded radical cations, this is not an unreasonable value, as even lower extinction coefficients have been reported for sterically constrained sulfur−sulfur bonded intermediates.[36a] The latter experiments demonstrate that intermediate $\mathbf{4a_2\text{-}SS}^+$ forms when possible, but that it is rather unstable even at high (4 mM) concentrations of thioether. Hence, the low yield of $\mathbf{4a_2\text{-}SS}^+$ under conditions where HO• radicals react with low concentrations (0.2 mM) of **4a** is not surprising.

To provide an alternative assessment of the species formed on pulse radiolysis of **2a**, **4a** and **8a**, computational studies were done. After identifying conformational minima, the radical cations were geometry optimized. In each case, both radical cations with S−O interactions and radical cations with S−N interactions were found. After simulating aqueous solvation using a continuum model, the electronic excitation

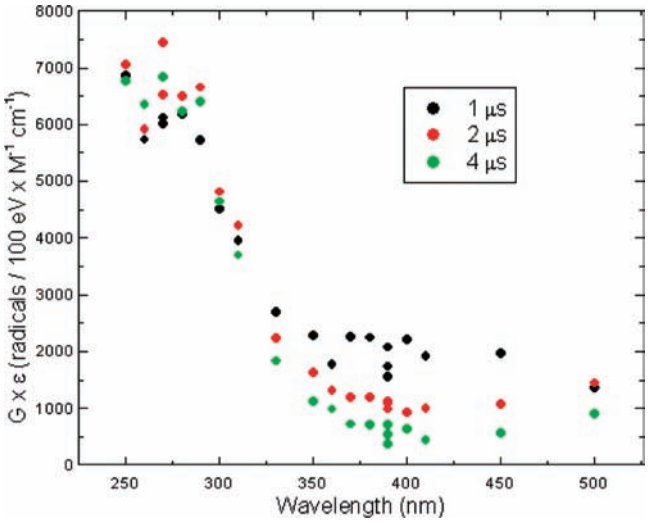

Figure 7. Time course at 1, 2, and 4 μs after pulse irradiation of 0.2 mM **8b** at pH 4.

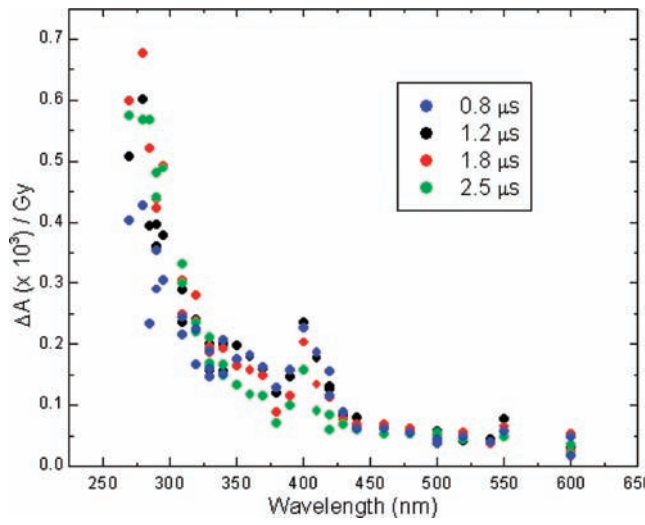

Figure 8. Experimental spectra (0.8, 1.2, 1.8, and 2.5 μs) after pulse irradiation of N_2O-saturated aqueous solution of 0.2 mM **4a** at pH 5.

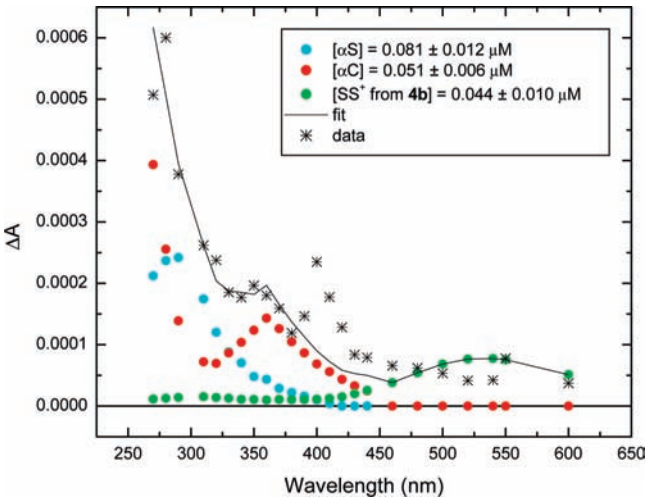

Figure 9. Experimental spectrum (*) of 0.2 mM **4a** at pH 5 in N_2O-saturated aqueous solution, 1.2 μs after pulse irradiation and fit using αS1/αS2, SS^+ and radical C•.

energies for each species were determined by time-dependent DFT calculations. The results are summarized in Table 2. In accord with the conclusions from pulse radiolysis studies, the SN^+ species (shown in the Supporting Information) are less stable than the corresponding SO^+ species (a rough estimate of the population of SN^+ species is less than 1% in every case). Two conformational minima were found for the SO^+ species in each case (see Figure 11) and the ratio of the two conformers based on relative SCF energies of the radical cations would be over 5:1 for **2a**, nearly 3:1 for **4a** and nearly 100:1 for **8a**. The computed optical absorption maxima for **2a** and **4a** are very similar (see Table 2) and are probably indistinguishable experimentally. Although the optical absorption maxima for the two conformers of **8a** differ significantly, there would be too little of the minor conformer to detect experimentally.

The SO^+ species are best described as 2c-3e bonded species with the unpaired electron in σ^*_{SO} as seen in the SOMOs for the lowest energy conformers of **2a**, **4a** and **8a** SO^+ species in Figure 12. Furthermore, the elongated S−O bond lengths (2.36−2.44 Å)[70] calculated for these species further support this bonding scheme. However, three different bonding schemes for sulfuranyl radicals have been suggested previously[71] in which the unpaired electron is in a σ, σ^* or π MO. For example, **11**[39a,c] and several Met-containing peptides[29a,c] which form S−O radical cations by one-electron oxidation and interaction between the sulfur and an amide oxygen, absorb with λ_{max} = 390 nm, and are suggested to be σ^*_{SO}-radicals, whereas **12** is suggested[71] to be T-shaped with the unpaired electron in an orbital perpendicular to the O, S, O, O plane and has an absorption maximum significantly blue-shifted from that of σ^*_{SO}-radicals. Radical **13** absorbs with λ_{max} = 390 nm (in CH_2Cl_2)[71] and was initially suggested to be a three-center, three-electron bond T-shaped species[72] but more recent theoretical studies suggest that it is a σ^*_{SO}-radical.[73] To determine if bonding possibilities other than 2c-3e bonding are possible for **2a-SO**$^+$, **4a-SO**$^+$ and **8a-SO**$^+$, calculations on T-shaped geometries for these species were geometry optimized. For **2a-SO**$^+$ and **4a-SO**$^+$, the σ^*_{SO}-radical geometry, previously found, was obtained. For **8a-**

Scheme 8

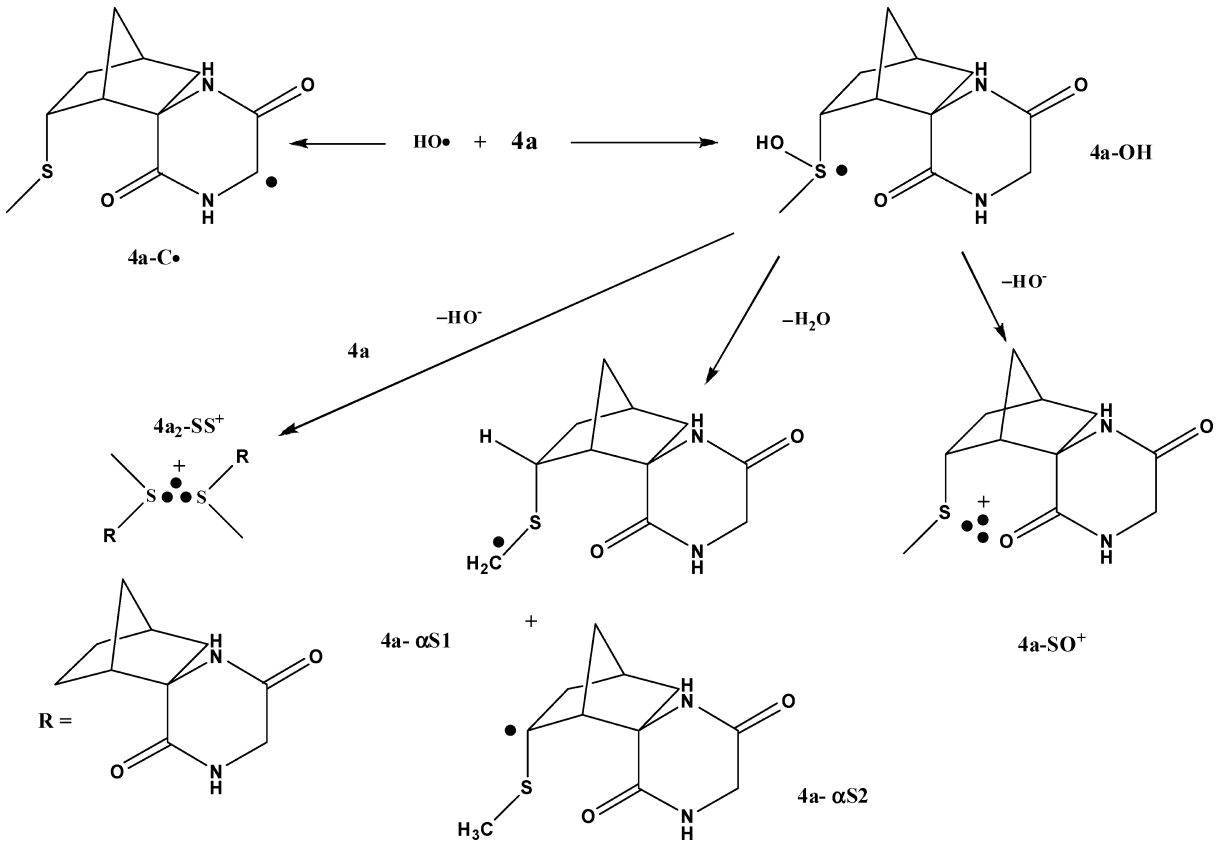

Scheme 9

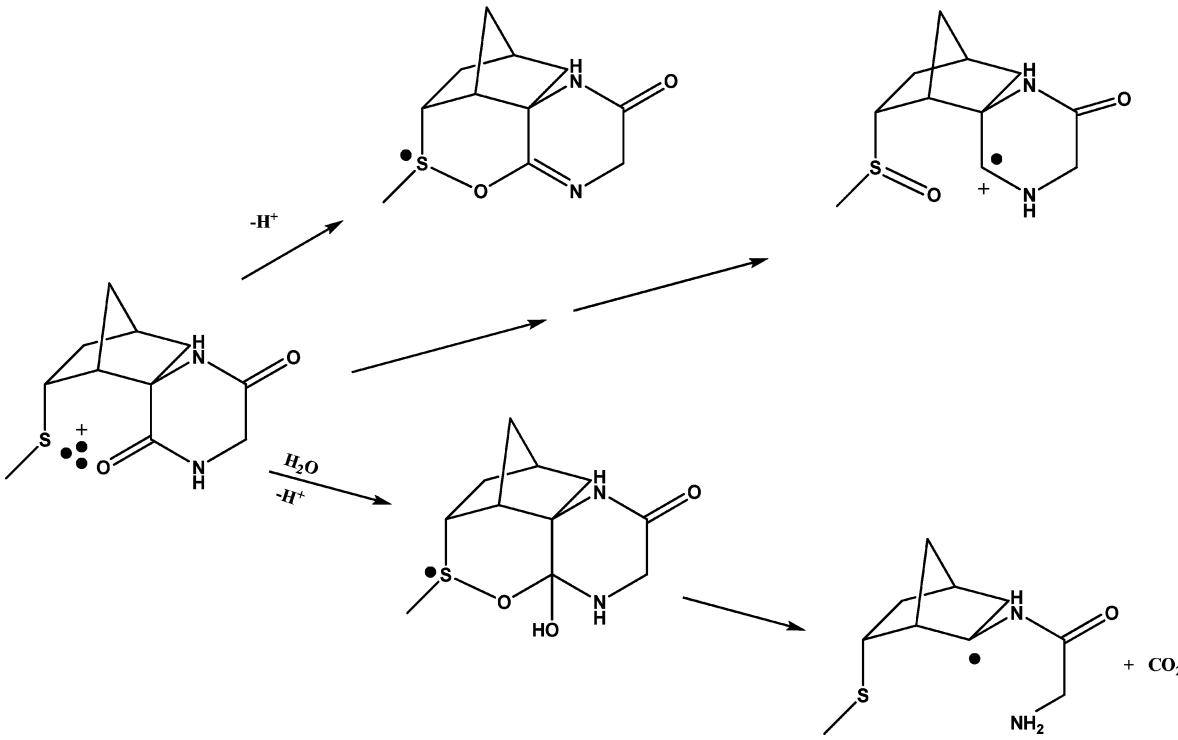

SO$^+$, T-shaped geometries were found but these were substantially higher in energy than the energies of the σ^*_{SO}-radicals.

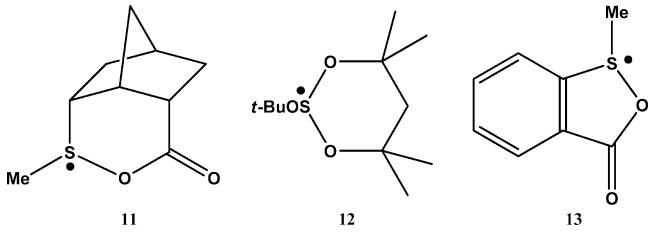

11 12 13

As already pointed out **2a-SO**$^+$ and **4a-SO**$^+$ decompose much more rapidly than **8a-SO**$^+$. It is known[36] that 2c-3e

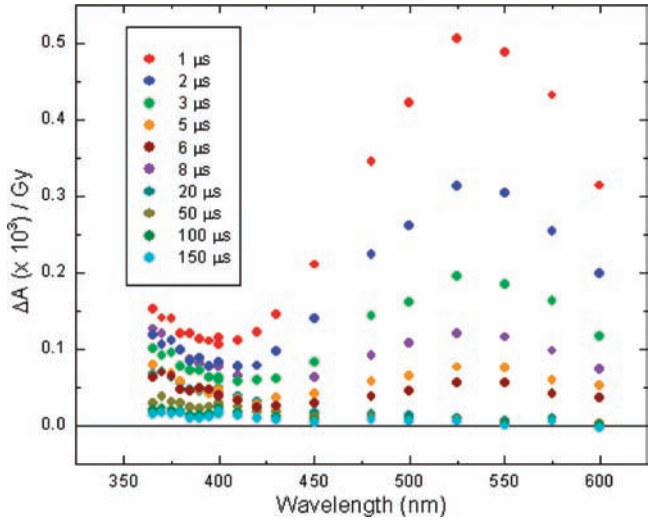

Figure 10. Experimental optical spectrum after pulse irradiation of an Ar-saturated aqueous solution of 4 mM **4a**, 5 mM $K_2S_2O_8$, 10 mM phosphate and 3 M *tert*-butyl alcohol at pH 4.

Table 2. Full Molecule Energies and Excitation Wavelengths for **2a**, **4a**, and **8a** Radical Cations

compound conformer[a]	rad. cat. rel. SCF energy (kcal/mol)	lowest excitation wavelength (oscillator strength)[b]	major excitation wavelength (osc. strength)[b]
2a *S−O endo*	1.97	480 nm (*0.0030*)	408 nm (*0.1507*)
2a *S−O exo*	0.00	464 nm (*0.0005*)	411 nm (*0.1418*)
2a *S−N*	7.14	646 nm (*0.0035*)	459 nm (*0.0609*)
4a *S−O endo*	1.23	525 nm (*0.0065*)	509 nm (*0.0562*)
4a *S−O exo*	0.00	576 nm (*0.0078*)	511 nm (*0.0318*)
4a *S−N*	8.12	1155 nm (*0.0013*)	894 nm (*0.0772*)
8a *S−O perp*	5.37	532 nm (*0.0028*)	498 nm (*0.0762*)
8a *S−O exo*	0.00	454 nm (*0.0075*)	422 nm (*0.0627*)
8a *S−N*	14.48	672 nm (*0.0083*)	468 nm (*0.0109*)

[a] The conformers labeled "exo" have $C_{Norbornyl\text{-}3}$-$C_{Norbornyl\text{-}2}$−S−C_{Me} dihedral angle of (very) roughly 180°, so that the methylthio group extends away from the bicyclic system, while the conformers labeled "endo" have a dihedral angle of less than 30°; however, in the **8a** conformer labeled "perp", the $C_{Norbornyl\text{-}1}$−$C_{Norbornyl\text{-}2}$−S−C_{Me} dihedral angle is less than 30°, making that conformer at roughly right-angles to all the others. [b] Oscillator strength is directly proportional to the *area* of an optical transition, but can be assumed to be roughly proportional to the molar absorptivity at λ_{max}, at least to the extent that the lowest-energy transitions, with their very small oscillator strengths, cannot be responsible for the observed experimental absorptions.

bonded species are more stable in five-membered rings than in six-membered rings. In **2a-SO**$^+$ and **4a-SO**$^+$ the 2c-3e SO bond is in a six-membered ring; whereas, it is in a five-membered ring in **8a-SO**$^+$. In addition, the unknown decomposition pathway for **2a-SO**$^+$ and **4a-SO**$^+$ may be

(70) The sum of the covalent single bond radii for S and O is 1.70 Å: Pauling, L. *The Nature of the Chemical Bond*; Cornell University Press: Ithaca, N.Y., 1960; p 224.
(71) Chatgilialoglu, C.; Castelhano, A. L.; Griller, D. *J. Org. Chem.* **1985**, *50*, 2516–2518, and references therein.
(72) Perkins, C. W.; Martin, J. C.; Arduengo, A. J.; Lau, W.; Alegria, A.; Kochi, J. K. *J. Am. Chem. Soc.* **1980**, *102*, 7753–7759.
(73) Pogocki, D.; Schöneich, C. *J. Org. Chem.* **2002**, *67*, 1526–1535.

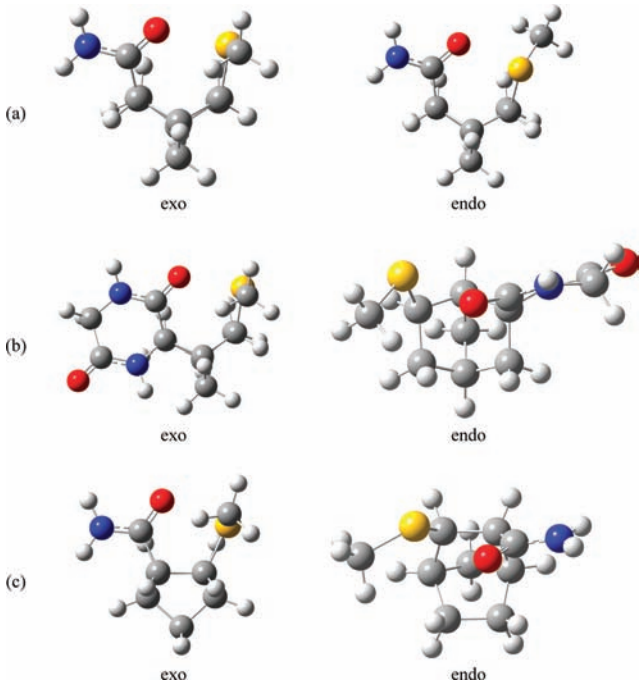

Figure 11. Drawings of structures for calculated energy minima for (a) **2a-SO**$^+$, (b) **4a-SO**$^+$, and (c) **8a-SO**$^+$.

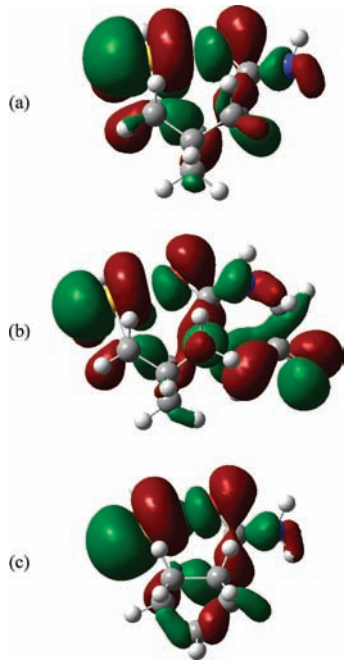

Figure 12. Plots of the SOMO for the lowest energy conformers of SO$^+$ species of (a) **2a**, (b) **4a** and (c) **8a**.

initiated by hydration of the activated amide moiety as shown in Schemes 4 and 9. This hydrated intermediate is analogous to the tetrahedral intermediate formed in the acid hydrolysis of amides[74] in which O-protonation is followed by hydration. Thus it is conjectured that the electron-deficient sulfur bound to the amide oxygen serves the same function as protonation in enhancing the electrophilicity of the amide moiety. Furthermore, hydration may be more favorable for **2a-SO**$^+$ and **4a-SO**$^+$ because many examples are known[75] in which addition to an sp^2-hybridized center is more favorable for a six-membered ring than for a five-membered ring. The proposed reason for this difference is that torsional strain is relieved in the former but increased in the latter.

Conclusions

In summary, neighboring amide participation has been shown to lower the electrochemical oxidation potential of thioethers. Pulse radiolysis studies of these conformationally restricted systems show unequivocally that one-electron oxidation results in initial S−O bond formation, not S−N, in agreement with previous studies on methionyl peptides.[12a,c,] DFT computational studies support the preferential formation of SO$^+$ rather than SN$^+$ species. The S−O bonding in the SO$^+$ species involves 2c-3e bonding (with the unpaired electron in σ^*_{SO}). Calculations also suggest that decomposition of **2a-SO**$^+$ and **4a-SO**$^+$ initiated by hydration accounts for the much longer lifetime of **8a-SO**$^+$ than **2a-SO**$^+$ and **4a-SO**$^+$. Thus neighboring amide participation on thioether oxidation could facilitate metal ion reduction by β-amyloid peptides.

Experimental Section

Spiro[(6-*endo*-methylthio)bicyclo[2.2.1]heptane-2,4′-imidazolidene]-2′,5′-dione(1*R*,2*R*,4*S*; 1*S*,2*S*,4*R*), 3. Trimethylsilylisocyanate (172 μL, 1.29 mmol) was added to methyl 2-*exo*-amino-6-*endo*-methylthiobicyclo[2.2.1]heptane-2-*endo*-carboxylate, **5**, (186 mg, 0.86 mmol), prepared as previously reported,[40] under nitrogen. The solution was heated under reflux for 2 h. The reaction mixture was cooled and the product precipitated from the solution as a white solid. The solvent was evaporated and crude material was used for the next step without purification.

The crude product was dissolved in anhydrous MeOH (1 mL) and anhydrous THF (0.7 mL), and freshly prepared NaOMe (1.6 mL, 0.86 mmol) was added to the reaction mixture. The reaction was stirred overnight. Solvents were rotary-evaporated and product was purified by silica gel chromatography using MeOH/CH_2Cl_2 solvent mixture as eluent to give **3** as a white solid (176 mg, 91%): ^{1}H NMR (500 MHz, CD_3OD) δ 1.38 (ddd, J = 20.5, 8.0, 2.0 Hz, 1H), 1.56 (dt, J = 10.5, 1.5 Hz, 1H), 1.70 (dd, J = 11.0, 2 Hz, 1H), 1.77 (m, 1H), 2.00 (dd, J = 9.5, 3 Hz, 1H), 2.03 (s, 3H), 2.12 (m, 1H), 2.39 (bs, 1H), 2.69 (m, 1H), 2.48 (s, 1H), 2.81 (m, 1H); ^{13}C NMR (125 MHz, CD_3OD) δ 18.56, 35.18, 38.42, 42.37, 46.34, 50.61, 56.39, 68.51, 158.7, 180.0; HRMS (FAB$^+$, *m*/*z*): Calcd. for $C_{10}H_{14}N_2O_2S\cdot H^+$, 227.0854; Found: 227.0863.

Spiro[(6-*endo*-methylthio)bicyclo[2.2.1]heptane-2,4′-piperazine]-3′,6′-dione(1*R*,2*R*,4*S*; 1*S*,2*S*,4*R*), 4a. To a solution of methyl 2-*exo*-amino-6-*endo*-methylthiobicyclo[2.2.1]heptane-2-*endo*-carboxylate, **5** (130 mg, 0.60 mmol), prepared as previously reported,[40] *N*-Boc-glycine (317 mg, 1.81 mmol) and DMAP (221 mg, 1.81 mmol) in CH_2Cl_2 (15 mL) was added 1,3-dicyclohexylcarbodiimide (374 mg, 1.81 mmol), and the reaction mixture was stirred for 40 h at room temperature. The precipitate was filtered and washed with CH_2Cl_2 (30 mL); the filtrate was washed with a saturated aqueous sodium bicarbonate solution (2 × 10 mL), dried ($MgSO_4$), and then concentrated *in vacuo*. The residue was purified on a silica gel column using hexane/ethyl acetate as eluent. The product was dissolved in ether, filtered to remove urea, and concentrated *in vacuo* to give a white solid (221 mg, 100% yield): ^{1}H NMR (500 MHz, $CDCl_3$) δ 1.02 (ddd, J = 19.5,

(74) (a) Brown, R. S.; Bennett, A. J.; Slebocka-Tilk, H. *Acc. Chem. Res.* **1992**, *25*, 481–488. (b) Brown, R. S. In *The Amide Linkage*; Greenberg, A., Breneman, C. M., Liebman, J. F., Eds.; Wiley: New York, 2000; Chapter 4. (c) Cox, R. A. *Can. J. Chem.* **2005**, *83*, 1391–1399.

(75) Bell, R. P. *Adv. Phys. Org. Chem.* **1966**, *4*, 1–29.

(76) Although SO$^+$ species are initially formed on one-electron oxidation of methionyl peptides they rearrange to neutral radicals with an S−N bond.

7.0, 1.5 Hz, 1H), 1.40 (s, 9H), 1.44 (d, J = 10.5 Hz, 1H), 1.73 (m, 1H), 1.88 (d, J = 10 Hz, 1H), 1.97 (s, 3H), 2.06 (m, 1H), 2.25 (bs, 1H), 2.57 (bs, 1H), 2.63 (dd, J = 13.5, 2.5 Hz, 1H), 2.99 (m, 1H), 3.64 (s, 3H), 3.67 (m, 2H), 5.46 (bs, 1H), 7.04 (bs, 1H); ^{13}C NMR (125 MHz, CD_3OD) 16.66, 28.22, 34.23, 37.08, 39.38, 42.68, 46.21, 50.29, 52.14, 64.13, 168.3, 172.9.

This intermediate (221 mg, 0.59 mmol) was dissolved in CH_2Cl_2 (2.5 mL) and TFA (1 mL) was added to the reaction mixture. The reaction was stirred for 1 h at room temperature, monitoring by TLC. A solution of NaOH (537 mg, 13.4 mmol) was added to reaction mixture to quench the TFA and then the reaction mixture was extracted with ethyl acetate to yield the product (159 mg, 100%): ^{1}H (500 MHz, $CDCl_3$) δ 0.97 (m, 1H), 1.56 (dd, J = 10.0, 1.0 Hz, 1H), 1.75 (dt, J = 7.0, 3.0 Hz, 1H), 1.95 (dd, J = 10.5, 1.5 Hz, 1H), 2.00 (s, 3H), 2.09 (m, 1H), 2.35 (bs, 1H), 2.61 (dd, J = 13.4, 2.5 Hz, 1H), 2.70 (bs, 1H), 3.11 (m, 1H), 3.59 (s, 2H), 3.65 (s, 3H), 4.96 (bs, 2H).

To the crude product (419 mg, 1.54 mmol) freshly prepared NaOMe (8.7 mL, 4.62 mmol) was added. The reaction was stirred for 72 h while monitoring by TLC. The solvent was evaporated and the compound was recrystallized from MeOH/CH_2Cl_2 to give **4a** as white crystals (370 mg, 100%); ^{1}H NMR (500 MHz, CD_3OD) δ 1.38 (ddd, J = 20.5, 8.0, 2.0 Hz, 1H), 1.53 (m, 1H), 1.70 (dd, J = 10.5, 1.5 Hz, 1H), 2.07 (s, 3H), 2.09 (m, 1H), 2.35 (bs, 1H), 2.52 (dd, J = 13, 3 Hz, 1H), 2.66 (bs, 1H), 2.95 (m, 1H), 3.75 (d, J = 17.5 Hz, 1H), 4.18 (d, J = 17.5 Hz, 1H); ^{13}C NMR (125 MHz, CD_3OD) δ 17.42, 34.53, 37.43, 40.41, 42.60, 46.43, 52.70, 64.29, 78.68, 171.4, 173.0; HRMS (FAB$^+$, m/z): Calcd. for $C_{11}H_{16}N_2O_2S\cdot H^+$, 241.1011; Found: 241.1004.

Spiro[(6-*endo*-methylthio)bicyclo[2.2.1]heptane-2,4′-piperazine]-5′,5′-dimethyl-3′,6′-dione(1*R*,2*R*,4*S*; 1*S*,2*S*,4*R*), 4b. To a solution of amino ester **5** (75 mg, 0.36 mmol), N-BOC-dimethyl-glycine (219 mg, 1.08 mmol), and DMAP (219 mg, 1.08 mmol) in CH_2Cl_2 (10 mL) was added DCC (222 mg, 1.08 mmol) and the reaction mixture was stirred for 28 h at 40 °C. Dichloromethane was evaporated and the residue was dissolved in ethyl ether; the precipitate was filtered and washed with ethyl ether (30 mL). The filtrate was washed with an aqueous saturated sodium bicarbonate solution (2 × 10 mL), dried ($MgSO_4$), and then concentrated in vacuo. The residue was purified on a silica gel column using hexane/ethyl acetate as eluent to give a white solid (89 mg, 61% yield): ^{1}H NMR (500 MHz, $CDCl_3$) δ 1.10 (m, 1H), 1.31 (s, 6H), 1.51 (d, J = 10.0 Hz, 1H), 1.63 (bs, 2H), 1.73 (dt, J = 13.0, 4.0 Hz, 1H), 1.93 (d, J = 10 Hz, 1H), 2.05 (s, 3H), 2.11 (m, 1H), 2.40 (bs, 1H), 2.64 (bs, 1H), 2.71 (dd, J = 13.5, 2.5 Hz, 1H), 3.05 (m, 1H), 3.72 (s, 3H), 7.96 (bs, 1H); ^{13}C NMR (125 MHz, $CDCl_3$) δ 16.69, 28.61, 28.82, 34.27, 37.16, 39.55, 42.91, 46.34, 50.33, 52.01, 54.52, 63.58, 172.9, 176.0.

Cyclization of this intermediate using the same procedure as that used in the synthesis of **4a** provided **4b**: ^{1}H NMR (500 MHz, CD_3OD) δ 1.41 (m, 1H), 1.43 (s, 3H), 1.48 (m, 2H), 1.57 (s, 3H), 1.88 (dd, J = 10.5, 2.0 Hz, 1H), 2.03 (s, 3H), 2.06 (m, 1H), 2.33 (bs, 1H), 2.48 (dd, J = 12.5, 3.0 Hz, 1H), 2.54 (bs, 1H), 2.85 (m, 1H); ^{13}C NMR (125 MHz, $CDCl_3$) δ 17.98, 27.41, 28.65, 32.65, 36.33, 39.83, 44.95, 49.01, 55.48, 56.34, 62.94, 170.2, 173.4; HRMS (TOF MS EI$^+$, m/z): Calcd. for $C_{13}H_{20}N_2O_2S$, 268.1245; Found 268.1245.

(*Z*)-3-Methylthiopropenoic acid amide, 9a. To a solution of (*Z*)-3-methylthiopropenoic acid **9c** (1.2 g, 10 mmol), prepared as reported,[42] in dried THF (30 mL) was added thionyl chloride (1.3 g, 11 mmol) and a catalytic amount of DMF with ice bath cooling. The reaction mixture was stirred at 5−10 °C for 7 h and then added dropwise to dried THF (80 mL) saturated with anhydrous ammonia at 0 °C. After stirring for 3 h the solvents were removed by rotary evaporation to afford a solid which was extracted with boiling CH_2Cl_2. The extract was evaporated and chromatographed on a silica gel column, eluting with EtOAc, to provide **9a** as a white solid (0.88 g, 74% yield): mp 109−111 °C; ^{1}H NMR ($CDCl_3$, 250 MHz) δ 2.37 (s, 3H), 5.57 (br, 2H), 5.83 (d, J = 10 Hz, 1H), 6.90 (d, J = 10 Hz, 1H); ^{13}C NMR ($CDCl_3$) δ (ppm) 19.82, 114.9, 149.2, 168.6.

3-*endo*-Methylthiobicyclo[2.2.1]heptane-2-*endo*-carboxamide, 8a. mCPBA (0.77 g, 4.5 mmol) was added to a solution of amide **9a** (0.50 g, 4.3 mmol) dissolved in CH_2Cl_2 (20 mL) and the solution was stirred at 0 °C for 2 h. The solvent was removed and the crude residue added to CH_2Cl_2 (20 mL) containing 1,3-cyclopentadiene (1.2 g, 18 mmol). This reaction mixture was stirred for 12 h at 0 °C, then concentrated on a rotary evaporator, dissolved in MeOH and stirred under an atmosphere of H_2, after adding 10% Pd/C (30 mg), for 6 h at 40 °C. The mixture was filtered through Celite and the filtrate concentrated to dryness. The residue was suspended in anhydrous CH_3CN (60 mL), cooled to 0 °C, and NaI (2.3 g, 15 mmol) and $BF_3\cdot Et_2O$ (1.8 g, 13 mmol) added. The mixture was stirred at 0 °C for 5 min and then at room temperature for 2 h. A saturated aqueous solution of $Na_2S_2O_3$ was added until the brown mixture turned yellow. This solution was extracted with CH_2Cl_2. The extracts were washed with aqueous Na_2CO_3, rotary-evaporated and chromatographed on silica gel, eluting with EtOAc:hexanes (1:1) to give **8a** as a white solid (0.35 g, 44% yield): mp 128−130 °C; ^{1}H NMR ($CDCl_3$, 500 MHz) δ 1.35−1.55 (m, 4H), 1.75−1.90 (m, 2H) 2.07 (s, 3H), 2.47 (s, 1H), 2.61 (s, 1H) 2.88 (dd, J = 4, 11 Hz, 1H), 3.15 (dd, J = 4, 11 Hz, 1H), 6.88 (br, 1H), 7.27 (br, 1H); ^{13}C NMR ($CDCl_3$) δ 16.60, 22.74, 23.98, 39.25, 42.22, 48.67, 50.19, 174.3.

2-*endo*-Acetamido-3-*endo*-methylthiobicyclo[2.2.1]heptane, 8b. (*Z*)-3-Methylthiopropenoic acid **9c**, prepared as reported,[42] was oxidized with *m*-chloroperoxybenzoic acid following the procedure reported above for the oxidation of **9a** to **10a** except that crude **10b** was separated from *m*-chlorobenzoic acid by column chromatography on silica gel (2:8 EtOAc:hexanes to remove *m*-chlorobenzoic acid, followed by 3% MeOH in EtOAc) to give sulfoxide **10b** as a gummy white residue in 86% yield: ^{1}H NMR (d_4-MeOH, 250 MHz) δ 2.85 (3H, s), 5.16 (1H, br), 6.42 (d, J = 10.3 Hz, 1H), 6.97 (d, J = 10.3 Hz, 1H); ^{13}C NMR ($CDCl_3$, 250 MHz) δ 40.8, 127.8, 157.6, 167.3; IR (neat) 2500−3000 (OH), 1705 (C═O), 1234 (S═O) cm^{-1}; HREIMS: Calcd for $C_4H_6O_3S$ (M+1) m/z 135.0116. Found: 135.0016.

3-*endo*-(Methylthio)bicyclo[2.2.1]heptane-2-*endo*-carboxylic acid, 8c. Cyclopentadiene (1.2 g, 18 mmol) was added to a solution of **10b** (0.45 g, 3.36 mmol) in CH_2Cl_2 and was stirred at 0 °C for 12 h. The subsequent steps of catalytic hydrogenation and sulfoxide reduction were performed in the same manner as those for the synthesis of **8a**, except the crude product was not washed with aqueous Na_2CO_3 but instead chromatographed with EtOAc:hexanes (1:1) and then recrystallized with EtOAc to give **8c** as a white solid (0.25 g, 40%): mp 106−108 °C; ^{1}H NMR ($CDCl_3$, 500 MHz) δ 1.35−1.55 (m, 4H), 1.93 (dd, J = 2, 8 Hz, 2H), 2.47 (s, br, 1H), 2.57 (s, br, 1H), 3.09 (ddd, J = 1, 3.5, 11 Hz, 1H), 3.18 (dd, J = 2.5, 11 Hz, 1H); ^{13}C NMR ($CDCl_3$, 250 MHz) δ 16.8, 22.6, 23.5, 39.4, 41.1, 41.8, 48.4, 49.9, 178.1; IR (KBr) 2953 (br, OH), 1705 (C═O) cm^{-1}; HREIMS: Calcd for $C_9H_{14}O_2S$ (M$^+$): m/z 186.0715. Found: 186.0712.

3-*endo*-(Methylthio)bicyclo[2.2.1]heptane-2-*endo*-carbobenzyloxyamine, 8d. A solution of **8c** (0.160 g, 0.90 mmol) in CCl_4 (9 mL) and triethylamine (0.180 g, 1.88 mmol) was refluxed for 15 min. DPPA (0.300 g, 1.01 mmol) and triethylamine (0.091 g, 0.90 mmol) were added and the reaction was refluxed for an additional 2 h. Benzyl alcohol (1.2 mL) was added and the reaction was refluxed overnight. The solvents were removed under reduced pressure and the mixture was chromatographed with EtOAc:hexanes (1:10) to obtain the desired carbamate as a slightly yellow oil (0.166 g, 66%): ^{1}H NMR ($CDCl_3$, 500 MHz) δ 1.35−1.55 (6H, m), 1.96 (3H, s), 2.47 (1H, s), 2.51 (1H, s), 3.12 (ddd, J = 1, 4, 10.5 Hz, 1H), 4.03 (1H, m), 5.11 (2H, s), 5.80 (d, J = 7.5 Hz, 1H), 7.29−7.38 (5H, m); ^{13}C NMR ($CDCl_3$, 300 MHz) δ 15.9, 21.0, 23.1, 37.1, 41.2, 42.1, 51.3, 51.6, 66.6, 128.0, 128.5, 136.6, 156.2; IR (neat) 3362

(NH_2), 1723 (C═O) cm^{-1}; HREIMS: Calcd for $C_{16}H_{21}NO_2S$ (M^+): *m*/*z* 291.1293. Found: 291.1305.

3-*endo*-(Methylthio)bicyclo[2.2.1]heptane-2-*endo*-acetamide, 8b. A solution of **8d** (0.122 g, 0.46 mmol) in MeOH (4 mL) and 40% aqueous KOH solution (2 mL) was refluxed for 6 h. Methanol was removed under reduced pressure and the crude mixture was extracted with EtOAc after the addition of water (4 mL). The organic layer was dried ($MgSO_4$) and rotary-evaporated to give a yellow oil which was dissolved in CH_2Cl_2 (3 mL). Triethylamine (0.174 g, 1.72 mmol) was added, followed by dropwise addition of acetyl chloride (0.122 g, 1.6 mmol). The reaction was stirred at room temperature for 3 h and saturated aqueous sodium carbonate was added. The basic solution was extracted with EtOAc and the extract was concentrated using rotary evaporation to give a yellow oil. The oil was column-chromatographed using EtOAc:hexanes (3:7) to give **8b** as a white solid (0.048 g, 52%): mp 71−73 °C; ^{1}NMR ($CDCl_3$, 300 MHz) δ 1.36−1.55 (6H, m), 2.00 (3H, s), 2.05 (3H, s), 2.46 (1H, s), 2.54 (1H, s), 3.12 (dd, J = 4, 10.5 Hz, 1H), 4.16−4.23 (1H, m), 6.53 (1H, br); ^{13}C NMR ($CDCl_3$, 300 MHz) δ 16.0, 21.1, 23.2, 23.3, 37.3, 41.0, 42.1, 49.4, 51.6, 169.9; IR (KBr) 3326 (NH), 1651 (C═O) cm^{-1}; HREIMS: Calcd for $C_{10}H_{17}NOS$ (M^+): *m*/*z* 199.1031. Found: 199.1039.

Electrochemistry. Anhydrous acetonitrile (99.8%, Sigma-Aldrich) was used directly without purification. Electrochemical measurements were carried out under nitrogen in a Scienceware glovebox. Tetra-*n*-butylammonium perchlorate and tetra-*n*-butylammonium hexafluorophosphate were obtained from Sigma-Aldrich and vacuum-dried. A three-compartment electrochemical cell (20 mL) was used for the cyclic voltammetric studies. The side arms contained the reference electrode (Ag/0.1 M $AgNO_3$ in acetonitrile) and a platinum counter electrode with a surface area of approximately 1 cm^2. Before each experiment, the platinum working disk electrode (2 mm diam.) was polished with alumina powder (1 and 0.3 μm), extensively washed with ultrapure water, acetone and then oven-dried. The electrochemical instrumentation was a potentiostat CH Instruments model CHI 620C connected to a computer for data acquisition.

Pulse Radiolysis. Pulse radiolysis experiments were performed on the Titan 8 MeV Beta model TBS 8/16−1S linear accelerator in the Radiation Laboratory at the University of Notre Dame, and on a Febetron 705 2 MeV accelerator (L-3 Communications, San Leandro, CA) in the Laboratory for Inorganic Chemistry at the Federal Institute of Technology in Zürich, Switzerland. The experimental setups have been described.[84]

Computations. Various potential conformers of **2a**, **4a** and **8a** were identified by Osawa search (using MacSpartan v1.0.2[77] and the PM3 semiempirical method[78]) and by chemical intuition and analogy. Each conformer was fully optimized using the B3PW91 hybrid DFT method[79] and employing the 6-31+G* basis.[80] Additionally, a self-consistent reaction field was applied to simulate aqueous solvation. A polarizable-continuum model (of the integral-equation formalism method type) was used[81] with the United-Atom method optimized for Kohn−Sham orbitals for solvent-cavity construction. The electronic excitation energies of each optimized conformer were then computed using time-dependent DFT (TD-B3PW91/6-31+G*) with nonequilibrium solvation (*same solvation model as before*). The computations were limited to considering doublet-spin species. Gaussian03[82] was used for all of the optimization and excitation calculations.

Acknowledgment. We gratefully acknowledge support of this work by the National Science Foundation (CHE-0455575). The X-ray crystal data for **4b** were collected at the University of Newcastle Upon Tyne by Dr. Ross Harrington and Professor William Clegg. This is Document No. NDRL 4807 from the Notre Dame Radiation Laboratory. The Notre Dame Radiation Laboratory is supported by the Office of Basic Energy Sciences of the U.S. Department of Energy.

Supporting Information Available: Complete refs 21b and 82, deconvolution of the spectrum of **2a** after pulse radiolysis fitting with S−N radical cation, alternative drawing of **4b** from X-ray crystal structure study, X-ray crystallographic parameters for **4b**, computational results including absolute energies and geometries for **2a-SO$^+$**, **4a-SO$^+$** and **8a-SO$^+$**. This material is available free of charge via the Internet at http://pubs.acs.org.

JA904895U

(77) Wavefunction, Inc., 18401 Von Karman Avenue, Suite 370, Irvine, CA 92612.

(78) Stewart, J. J. P. *J. Comput. Chem.* **1989**, *10*, 209–220. Stewart, J. J. P. *J. Comput. Chem.* **1989**, *10*, 221–264.

(79) B3: Becke, A. *J. Chem. Phys.* **1993**, *98*, 5648–5652. PW91: Burke, K.; Perdew, J. P.; Wang, Y. In *Electronic Density Functional Theory: Recent Progress and New Directions*; Dobson, J. F., Vignale, G., Das, M. P., Eds.; Plenum: New York, 1998; Perdew, J. P. In *Electronic Structure of Solids '91*; Ziesche, P., Eschrig, H., Eds.; Verlag: Berlin, 1991; chapter 11; Perdew, J. P.; Chevary, J. A.; Vosko, S. H.; Jackson, K. A.; Pederson, M. R.; Singh, D. J.; Fiolhais, C. *Phys. Rev. B* **1992**, *46*, 6671–6687. Perdew, J. P.; Chevary, J. A.; Vosko, S. H.; Jackson, K. A.; Pederson, M. R.; Singh, D. J.; Fiolhais, C. *Phys. Rev. B* **1993**, *48*, 4978. Perdew, J. P.; Burke, K.; Wang, Y. *Phys. Rev. B* **1996**, *54*, 16533–16539.

(80) Ditchfield, R.; Hehre, W. J.; Pople, J. A. *J. Chem. Phys.* **1971**, *54*, 724–728. See also, for example: Rassolov, V. A.; Ratner, M. A.; Pople, J. A.; Redfern, P. C.; Curtiss, L. A. *J. Comput. Chem.* **2001**, *22*, 976–984.

(81) Cancès, E.; Mennucci, B. *J. Chem. Phys.* **2001**, *114*, 4744–4745.

(82) Frisch, M. J.; et al. *Gaussian 03, Revision D.01*; Gaussian, Inc.: Wallingford, CT, 2004.

(83) Bobrowski, K.; Hug, G. L.; Marciniak, B.; Schöneich, C. *J. Am. Chem. Soc.* **1997**, *119*, 8000–8011.

(84) Hug, G. L.; Wang, Y.; Schöneich, C.; Jiang, P.-Y.; Fessenden, R. W. *Radiat. Phys. Chem.* **1999**, *54*, 559–566.